Reliability Engineering and System Safety 243 (2024) 109895

Contents lists available at ScienceDirect

Reliability Engineering and System Safety

journal homepage: www.elsevier.com/locate/ress

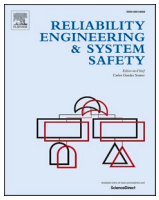

# Vulnerability Assessment of Industrial Sites to Interface Fires and Wildfires

Federica Ricci [a], Alessio Misuri [a], Giordano Emrys Scarponi [a], Valerio Cozzani [a,*], Micaela Demichela [b]

[a] LISES – Laboratory of Industrial Safety and Environmental Sustainability, DICAM - Department of Civil, Chemical, Environmental and Material Engineering, University of Bologna, via Terracini 28, 40131 Bologna, Italy
[b] SAfeR, Department of Applied Science and Technology, Politecnico di Torino, Corso Duca degli Abruzzi, 24, 10129 Torino Italy

ARTICLE INFO

*Keywords:*
Wildfire
Interface Fire
Natech
Cascading events
Domino effect
Dynamic Vulnerability Assessment
Risk Assessment

ABSTRACT

In the framework of climate change, the hazard caused by wildfires approaching the anthropic settlements is raising an increasing concern. Fatalities and relevant damage to properties were recently caused by wildfires affecting the Wildland-Urban and Wildland-Industrial Interfaces. Industrial sites storing large quantities of hazardous materials are vulnerable to interface fires, which have the potential to trigger specific cascading events such as Natech scenarios followed by domino effects. The present study aims at providing a methodology for the quantitative assessment of the vulnerability of industrial sites exposed to wildfires. The approach provides a novel framework for the identification and quantification of all the chains of failures that may occur due to wildfires or interface fires approaching industrial sites. The methodology accounts for the thermal radiation from fires in both primary Natech scenarios and cascading scenarios triggered by domino effects. The dynamic features of interface fires and the synergistic effects of multiple fires are also taken into account. The results of a case study demonstrated the importance of considering the dynamic behavior of wildfire, which strongly affects the vulnerability of industrial structures. The results also evidence the importance of emergency management and first response on the overall vulnerability figures.

## 1. Introduction

The destructive interactions between natural events and industrial installations have become a matter of growing concern in the last decades [1,2]. Severe accidents may arise when natural hazards impact on installations where large amounts of hazardous substances are stored, as in the case of chemical and oil & gas facilities [3–6]. Technological accidents caused by the action of natural events are usually referred to as Natech accidents [7,8]. According to previous studies, around 5% of the events recorded in industrial accident databases are triggered by natural disasters [9,10]. This figure is probably even higher nowadays, as the number of Natech accidents reported in more recent studies is growing [11–13], and will possibly continue to rise due to the reduction in the return period of climate-related extreme natural events, as storms and floods [14,15]. Indeed, climate changes may cause modifications of extreme weather and climate events in terms of frequency, intensity, spatial extent, and duration, leading to natural events of unprecedented severity [16] or to low-intensity natural events, as cold and heat waves, affecting areas where such events are not usually recorded [17,18].

Several areas all over the world have experienced more intense and longer droughts in recent years, and the likelihood of such events is foreseen to increase year by year due to climate change [16]. According to Jolly et al. [19], fire weather seasons have lengthened by about 19 % between 1979 and 2013, further increasing wildfire risk and severity, influencing fire regimes and promoting the conditions for the ignition and the rapid spread of forest fires [20–22]. An increase in both the number of large fires [23] and the extension of burned areas [24,25] have been documented over the last decades across the western United States of America (US) and in other fire-prone areas [26,27]. Data from the US National Interagency Fire Center [28], highlighting the increase in the average burned area per fire reported confirm this trend [28].

The expansion of Wildland-Urban Interfaces (WUIs) and Wildfire-Industrial Interfaces (WIIs) fostered by urban and industrial development in rural areas [29,30] increases the likelihood of forest fires affecting anthropic settlements. Interface fires occurring at WUIs pose complex challenges concerning the management of fire mitigation and civil protection [31], due to the possible presence of flammable materials such as fuel storage units in residential, commercial, or industrial areas [32–35] representing a relevant source of hazard. Recently,

* Corresponding author:
*E-mail address:* valerio.cozzani@unibo.it (V. Cozzani).

https://doi.org/10.1016/j.ress.2023.109895
Received 21 August 2023; Received in revised form 19 November 2023; Accepted 16 December 2023
Available online 17 December 2023

**Nomenclature**

| Symbol | Definition (Unit of measure) |
|---|---|
| A | First coefficient for the probit variable calculation (-) |
| B | Second coefficient for the probit variable calculation (-) |
| C | Death probability (-) |
| $D_v$ | Distance between wildfire and target (m) |
| de | Domino effect (-) |
| d | Damage distance (-) |
| $E_{wf}$ | Emissive power of the wildfire (kW/m$^2$) |
| f | Simple frequency (1/y) |
| F | Cumulated frequency (1/y) |
| $F_{wf\rightarrow i}$ | View factor from the wildfire to the generic *i-th* target (-) |
| HI | Hazard index (-) |
| $H_v$ | Height of trees (considering forest as vegetation) (m) |
| i | Index for generic target (-) |
| $IR_{j\rightarrow i}$ | Incident radiation from the *j-th* tank fire to the generic *i-th* target (kW/m$^2$) |
| $IR_{wf\rightarrow i}$ | Incident radiation from the wildfire to the generic *i-th* target (kW/m$^2$) |
| j | Index for generic emitter (-) |
| k | Index for generic branch/scenario (-) |
| L | Lethality (-) |
| $L_f$ | Flame length (m) |
| LHI | Layout hazard index (-) |
| LSIR | Local-specific individual risk (1/y) |
| MVT | Most vulnerable target (-) |
| N | Number of fatalities (-) |
| $n_T$ | Number of targets (-) |
| P | Probability of the branch/combined scenario (-) |
| $p_f$ | Failure probability of the equipment item (-) |
| $P_f$ | Overall failure probability (-) |
| PLL | Potential life loss (1/y) |
| **S** | Status vector (-) |
| SD | Safety distances between vegetation and targets (m) |
| SEI | Synergistic effect index (-) |
| t | Time (s) |
| TD | Thermal dose (kJ/m$^2$) |
| $TD_C$ | Critical thermal dose (kJ/m$^2$) |
| $T_f$ | Flame black body temperature (K) |
| TR | Overall thermal radiation received by a target (kW/m$^2$) |
| ttf | Time to failure (s) |
| $t_{wf}$ | Maximum exposure time to wildfire (s) |
| UHI | Unit hazard index (-) |
| V | Volume of the tank (m$^3$) |
| $W_f$ | Fire-front width (m) |
| wf | Wildfire (-) |
| X | Generic adverse dose for probit variable calculation (-) |
| Y | Probit variable (-) |
| α | Coefficient in thermal dose calculation *(1.128 in the present study)* (-) |
| β | Parameter *(0 for protected tanks, 1 otherwise)* (-) |
| δ | Parameter *(1 for active fires, 1 otherwise)* (-) |
| γ | Parameter *(1 for reference intervention time, 2 for delayed intervention time)* (-) |
| θ | Flame tilt angle (rad) |
| $\tau_a$ | Atmospheric transmissivity (-) |

attention has expanded to WII fires, with a focus on oil refineries and chemical plants, in which fire events (including wildfires) may trigger domino scenarios [36–39] with severe consequences on people and assets. The provision of clearance areas from vegetation is usually adopted as a protection measure to prevent the fire from affecting industrial installations [40–44]. However, a recent study by Ricci et al. [45] evidenced that the safety distances prescribed by international standards and national regulations may not be sufficient to provide adequate protection against equipment damage and accident escalation in case of severe wildfires, highlighting the need for tools enabling a systematic assessment of the risk of Natech events triggered by wildfires.

A general framework for the quantitative risk assessment of Natech events was proposed by Cozzani et al. [46] and was successfully applied to the analysis of accident scenarios induced by earthquakes, floods, and lightning [47–49]. Recently, Khakzad et al. [50,51] exploited Bayesian networks to develop an approach for the quantitative assessment of the risk of Natech events caused by wildfires in oil facilities, addressing critical aspects such as the revenue loss due to operational shutdown. Other authors focused on the analysis of the resilience of electrical power lines [52] and road traffic networks in case of wildfires [53]. However, a method addressing the quantitative vulnerability and risk assessment of industrial sites to the specific cascading accidents potentially triggered by wildfires or interface fires is still lacking.

Wildfire potential impact on process and storage equipment items mainly occurs due to thermal radiation, as the presence of prescribed clearance areas should avoid flame engulfment [54,55]. However, atmospheric storage tanks have a high structural vulnerability to fire radiation [56] and are among the equipment items that are most likely to be exposed to an approaching wildfire or interface fire front, since they are usually installed in the external areas of industrial sites. Thus, assessing the vulnerability of this category of storage units to radiation from forest fire front is relevant to evaluate the likelihood of Natech scenarios involving tank farms caused by interface fires or wildfires.

In the present study, an innovative approach to the dynamic quantitative vulnerability assessment of atmospheric tank farms in wildfire scenarios was developed. The methodology takes into account both the primary Natech accidents directly generated by radiation from the wildfire and the potential escalation scenarios caused by domino effects. An original framework is defined for the identification and quantification of the cause-consequence chain of the cascading scenarios. A specific approach is adopted to capture the synergistic effect of multiple simultaneous fires, also considering the time evolution of the sequence of events.

Section 2 describes the methodology developed. A case study is defined in Section 3. Section 4 reports the results of the case study assessment also addressing the influence on equipment vulnerability of the intervention time of emergency teams. Section 5 includes a discussion of the results. Finally, in Section 6 the main conclusions of the study are reported.

## 2. Methodology

The methodology proposed for the quantitative assessment of the vulnerability of atmospheric tank farms to Natech scenarios triggered by fire radiation generated by wildfire is outlined in Fig. 1. The main aim of the procedure is the calculation of the vulnerability (expressed as the probability of damage) of the atmospheric tanks exposed to a wildfire of a given intensity, accounting for both the direct damage of the wildfire and the secondary scenarios generated by domino effect.

The relevant wildfire features (e.g. radiation intensity, duration, etc.) are intended as input data for the procedure since the wildfire modeling is out of the scope of the present methodology. However, a simplified approach is proposed to obtain conservative preliminary data on wildfire intensity, that may be applied in the absence of detailed modeling of wildfires affecting the site of interest. The data obtained from the simplified procedure may be used to obtain a preliminary assessment of

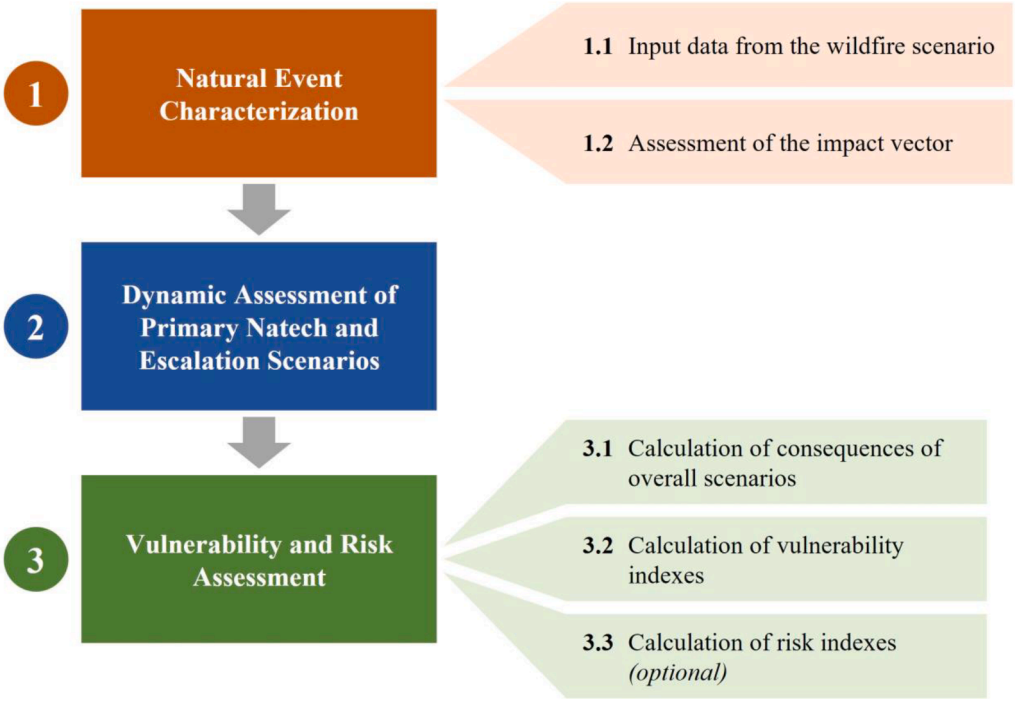


**Fig. 1.** Flowchart of the methodology developed for the quantitative assessment of vulnerability to Natech scenarios triggered by wildfires.

the vulnerability to wildfires, useful to understand the actual relevance of wildfire hazard on the site and the need to promote more accurate studies.

Even if the primary aim of the methodology is not the assessment of risk for the population, in case data are available for wildfire frequency and intensity, the procedure may be used as well to obtain individual and societal risk indexes. Since evacuation in the presence of wildfires may be a controversial issue [57], the assessment of these indexes provides baseline data, relevant in case evacuation or safe sheltering of the population and workers are not possible.

The methodology is based on an innovative dynamic event tree procedure that accounts for the thermal radiation from wildfires and related cascading scenarios. The methodology can be summarized in three main parts, as reported in Fig. 1. A detailed description of each step is provided in the following, highlighting the main features required to include the specific issues posed by Natech scenarios triggered by wildfires.

### 2.1. Natural event characterization

The natural event characterization consists of two steps: the collection of the input data needed to characterize the wildfire scenario and the assessment of its impact vector on the relevant targets, as shown in Fig. 1. More details on each step are reported in the following sections.

#### 2.1.1. Characterization of the wildfire scenario

The application of the methodology requires the following data to be obtained from the modeling of the wildfire scenario: *(i)* flame shape, *(ii)* flame dimensions, *(iii)* flame emissive power, and *(iv)* fire duration.

These parameters may be obtained from detailed site-specific modeling of the relevant wildfire scenario. Several methods were developed in the literature for forest fire hazard and risk evaluation [58], based on the application of statistical and data-mining models [59,60], machine learning models [61,62] or ensemble models [63,64]. Many software tools are also available to model wildfire behavior, such as PROMETHEUS [65], SPARK [66], and FARSITE [67]. These allow for the evaluation of fire propagation throughout vast wildland areas, both in terms of spreading rate and intensity. Alternatively, a detailed representation of the wildfire front can be achieved as well using advanced numerical tools (e.g. the Wildland Urban Interface Fire Dynamics Simulator by NIST [68]). However, several factors characterizing the burning vegetation, the weather conditions, and the morphological aspects of the territory need to be assessed and provided as input in order to apply such models. Moreover, such models are not intended to specifically address the local variations in the vegetation distribution and wind profile which may affect an interface fire or a wildfire approaching the edge of the vegetation [33]. These aspects are particularly relevant when considering wildfires affecting the wildland-industrial interface, where border effects become important, and the propagation is strongly affected by site-specific factors [32]. Thus, the detailed characterization of the wildfire hazard event under analysis can be obtained by the application of these methodologies and tools.

However, in case a detailed characterization of the wildfire is not available for the site of concern, simplified approaches may be adopted to obtain a conservative assessment of the potential wildfire scenario affecting the site. Simplified methods for wildfire characterization available in the literature typically use a solid flame model to represent the fire front and require a limited number of input data [45,69–71]. The application of such approaches is useful to obtain a preliminary screening of the relevance of the issue in the site of interest, based on suitable representation of the reference wildfire scenario.

In the present study, the simplified approach proposed by Ricci et al. [45] is suggested since it allows to characterize the fire front based on the vegetation type that surrounds the industrial area. A solid flame model is used to represent the fire front, as shown in Fig. 2. The fire front is modeled as a rectangular surface with one side equal to $L_f$ (flame length) and the other equal to $W_f$ (fire-front width), inclined of a tilt angle $\theta$ to the ground, with emissive power $E_{wf}$.

The flame shape and dimensions as well as its emissive power are an input to the model. These parameters are strongly dependent on the type of vegetation and its surface density, as well as on the weather conditions, which are characterized by seasonal variability and may change considerably over the lifetime of an industrial plant. Empirical formulas are available to estimate the geometric characteristics of the flame based on the heat release rate of the burning vegetation [72]. In the lack of

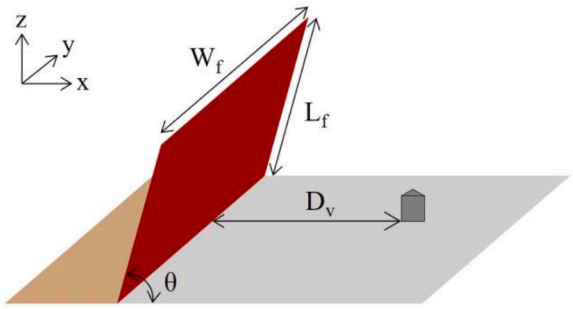


**Fig. 2.** Representation of the flame shape and size. $L_f$: flame length, $W_f$: fire-front width, $D_v$: distance between wildfire and target, $\theta$: flame tilt angle.

more specific information, the present methodology suggests adopting the assumptions discussed below, based on wildfire impact assessment studies available in the literature.

Wildfire maximum flame temperatures in the range 949 ÷ 1457 K are reported by [73], while in the experiment carried out by Finney and co-workers [74], temperatures recorded at the edge of spreading and stationary fires fluctuated from nearly ambient to over 1273 K. Thus, as suggested by several authors [69,70,75], a flame black body temperature of 1200 K can be considered, which corresponds to a flame emissive power of 118 kW/m$^2$.

The fire-front width $W_f$ may be assumed as infinite (the thermal radiation at the distances of interest do not increase significantly for values wider than 20 m [69]), the value of the tilt angle $\theta$ is the one that maximizes the view factor (and therefore the incident radiation on targets) and the flame length $L_f$ is calculated on the base of type of vegetation growing in the proximity of the plant boundary using Eq. (1), where $H_v$ is the height of the trees when considering forests [45].

$$L_f = \begin{cases} 7.5 & \text{Grassland fire} \\ 13 & \text{Shrubland fire} \\ 3.5 \cdot H_v & \text{Crown fire} \end{cases} \quad (1)$$

With respect to wildfire duration, it is necessary to evaluate the maximum duration for which industrial items are exposed to radiation from the fire. Even if the value is a function of several factors (e.g., slope of terrain, characteristic of the vegetation, meteorological conditions), the maximum exposure time might not exceed 15 min when considering fires at the edge of the vegetation [45,74].

Clearly enough, based on the knowledge of specific characteristics of the vegetation present in the proximity of the industrial installation under assessment, different values with respect to those suggested above can be adopted for the flame shape and dimensions as well as its emissive power and duration [76,77].

#### 2.1.2. Assessment of wildfire impact vector

The second step requires the assessment of the wildfire impact on targets (Step 1.2 in Fig. 1). As reported previously, the impact vector considered in the present study is the thermal radiation from wildfires on industrial installations. Thus, for the generic *i-th* target, the impact vector assessment requires the calculation of the incident radiation, $IR_{wf \to i}$, that is evaluated according to Eq. (2):

$$IR_{wf \to i} = E_{wf} \cdot F_{wf \to i} \cdot \tau_a \quad (2)$$

where $E_{wf}$ is the wildfire emissive power (kW/m$^2$), $F_{wf \to i}$ is the view factor between the wildfire and the *i-th* tank (dimensionless), and $\tau_a$ is the atmospheric transmissivity (dimensionless), assumed equal to 1 (as in several previous studies, e.g., see [69–71]). According to the flame shape considered in the present study (see Fig. 2), the view factor can be calculated using the model proposed by Mudan [78].

### 2.2. Dynamic assessment of primary Natech and escalation scenarios

The flowchart of the detailed procedure applied for the dynamic assessment of primary Natech and escalation scenarios (Step 2 in Fig. 1) is reported in Fig. 3. The dynamic approach is based on the definition of the event tree which considers the time-dependent chain of failures due to thermal radiation from wildfire and fires in atmospheric tanks.

The dynamic event tree is evaluated based on a procedure that requires the definition of three vectors: *i)* the status vector, ***S***, the elements of which represent the status of the corresponding target; *ii)* the thermal radiation vector, ***TR***, the elements of which represent the thermal radiation on the corresponding target, and *iii)* the thermal dose vector, ***TD***, in which each element corresponds to the thermal dose received by the corresponding target. Each vector includes a total of $n_T$ elements representing a possible target vessel (i.e., atmospheric tank).

Each element of ***S*** represents the status of the *i-th* target, and it can assume four alternative values (or states):

- *Vulnerable*: the *i-th* target is intact and, when exposed to fires, it may either fail or be protected by emergency teams.
- *Protected*: emergency teams were able to secure the *i-th* target before failure. The "*protected*" status is permanent. Hence, a protected target on a given event tree branch cannot change its state along the connected sub-branches.
- *Failed*: the *i-th* target is failed. This status is associated with the targets whose failure is not able to trigger a domino effect, e.g., a tank releasing a non-flammable liquid. Targets in the "*failed*" status do not influence the thermal radiation vector ***TR***. As for the "*protected*" status, also the "*failed*" status is permanent.
- *On fire*: the *i-th* target fails. This status is associated with the targets whose failure has the potential to trigger domino effects, e.g., a tank releasing a flammable liquid. Tanks in the "*on fire*" status modify the thermal radiation vector ***TR***.

The procedure also requires the definition of a scalar that represents the time, *t*, considered starting from the time at which the wildfire approaches the plant boundary.

In the first iteration of the methodology, starting values of the status vector ***S***, the thermal dose vector ***TD***, and the current time *t* should be assigned. Specifically, each element of ***S*** is set to "*vulnerable*", while those of ***TD*** are equal to 0. In addition, the current time *t* is set to 0.

Then, an iterative procedure was developed for the definition and quantification of the event tree, and the main features of each step are reported in the following sections. The procedure continues until all possible chains of failures are considered, based on the dynamic assessment of wildfire impact and fires from atmospheric equipment items.

#### 2.2.1. Thermal radiation vector calculation

In order to calculate the thermal radiation on each target, the incident radiations from the wildfire and each of the pool fires possibly caused by the failure of an atmospheric tank in the tank farm are considered in Eq. (3). Regardless of the method used for wildfire characterization (whether detailed or simplified, as discussed in Section 2.1.1), an average value of radiation may be obtained, that may be considered constant throughout the entire period of exposure to the fire. As for the pool fires, these are considered for the sake of simplicity the only credible scenario following the release of flammable substances from atmospheric tanks. This assumption is also justified by the high probability of immediate ignition due to the presence of an external fire. Moreover, the pool fires caused by tank failure are assumed to generate stationary radiation for a maximum duration corresponding to the time needed to burn all the tank inventory, estimated considering the burning rate reported by Mannan [79].

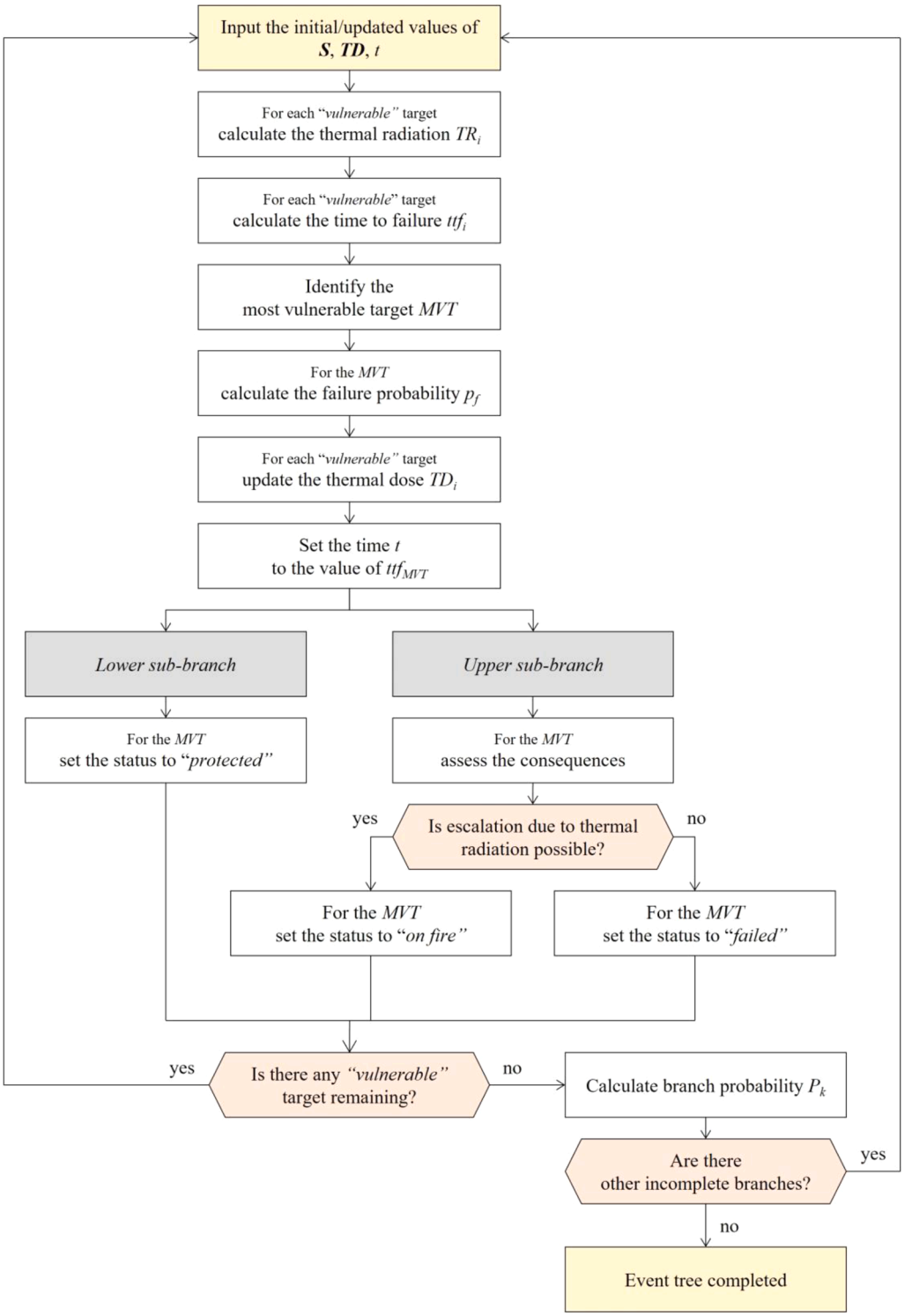


**Fig. 3.** Flowchart of the core of methodology for the definition of the event tree considering the dynamic chain of failures due to thermal radiation from wildfire and fires in atmospheric tanks. ***S**: status vector; **TD**: thermal dose vector; t: time.*

$$TR_i = IR_{wf\to i}\cdot\delta_{wf} + \sum_{j=1}^{n_T} IR_{j\to i}\cdot\delta_j \tag{3}$$

where $IR_{wf\to i}$ is the thermal radiation on the *i-th* target from the wildfire, $IR_{j\to i}$ is the thermal radiation on the *i-th* target from the *j-th* item, $n_T$ is the total number of tanks considered in the analysis, and $\delta$ is a parameter set to 1 if the status of the fire is active, and to 0 otherwise. Clearly enough, the calculation of the thermal radiation is performed only for tanks in "*vulnerable*" status.

### 2.2.2. Time to failure calculation

The calculation of the time to failure *ttf* for a generic *i-th* target tank is carried out applying the method of Zhou et al. [80]. The method allows capturing the dynamic and synergistic effect of multiple fires starting and ending at different times. It is based on the comparison of a thermal dose $TD_i$ [81] to a critical thermal dose $TD_{C,i}$ required to induce the

failure of the tank. The thermal dose received by the *i-th* target, $TD_i$, and the related critical thermal dose, $TD_{C,i}$, are defined as follows:

$$TD_i = \int_{t_1}^{t_2} TR_i^{\alpha} \cdot d\tau \tag{4}$$

$$TD_{C,i} = \exp\left(-2.667 \cdot 10^{-5} \cdot V + 9.877\right) \tag{5}$$

where $TR_i$ is the overall value of the thermal radiation received by the target (calculated according to Eq. (3) in the present approach), $\tau$ is time, $t_1$ and $t_2$ are the initial and final values of the time interval of interest, $\alpha$ is a constant (equal to 1.128 for atmospheric tanks in the present approach), and $V$ is the volume of the tank. It is worth mentioning that the values of $\alpha$ and $TD_{C,i}$ are derived from the correlations developed by Landucci et al. [37].

Thus, the time to failure of the *i-th* target is evaluated according to the following equation:

$$ttf_i = t + \frac{TD_{C,i} - TD_i}{\frac{1}{ttf_i - t} \cdot \int_t^{ttf_i} TR_i^{\alpha} \cdot d\tau} \tag{6}$$

The $ttf_i$ refers to the time elapsed between the moment in which the wildfire approaches the plant boundary and the failure of the tank. Noteworthy, Eq. (6) considers the average thermal radiation received by the *i-th* target in the time interval between $t$ and its time to failure, $ttf_i$, thus accounting for the variation in the thermal radiation that occurs when a fire ends.

### 2.2.3. Identification of the most vulnerable target and calculation of its failure probability

The target that features the lowest time to failure is identified as the most vulnerable target *MVT*. Following the approach proposed in several studies available in the literature [37,80,82,83], the calculation of the failure probability $p_f$ of the *MVT* is carried out using a probit model:

$$Y = A + B \cdot \ln(X) \tag{7}$$

where $Y$ is the probit variable, $A$ and $B$ are coefficients, and $X$ represents the adverse dose impacting the target. In the case of fire-induced domino effects, Landucci et al. [37] proposed to estimate the probit value based on the time to failure (i.e., posing $X = ttf$ in Eq. (7)) and to derive the parameters $A$ and $B$ comparing the $ttf$ with the characteristic times required for the intervention of emergency teams. Landucci et al. [37] also proposed general reference values for the probit coefficients, calculated assuming a 10% probability of successful mitigation within 5 min since the beginning of the fire and a 90% probability after 20 min. However, it is important to remark that these reference probabilities of successful mitigation were proposed considering the case of a tank exposed to a single fire in a conventional accident scenario. During wildfires and wildfire-induced accidents, several factors such as the harsh conditions caused by smoke, the need to contrast different simultaneous fire fronts, and the possible shortage of firefighting materials may hamper the emergency response, lowering the probability of successful mitigation and/or delaying the time after fire start at which successful mitigation actions are deployed. Landucci et al. [84] developed an approach to consider the influence of a harsh environment on the delay of first response and mitigation actions. In order to assess the importance of such factors, an additional set of reference values was introduced to account for possible delays in the intervention time. In accordance with the approach suggested by Bucelli et al. [85], the harsh conditions caused by the wildfire were considered to delay the response time, thus modifying the coefficient in Eq. (7). In the present study, for exemplification purposes, the harsh environment generated by the wildfire was considered to double the response time. Thus, a factor $\gamma$ equal to 2 was applied to the reference time values proposed by [37], not modifying the probability of successful mitigation corresponding to the two extremes of the interval. Table 1 shows the probit coefficients obtained considering the modification in the intervention time.

### 2.2.4. Update of the thermal dose and of the time step

The time to failure corresponding to the most vulnerable target $ttf_{MVT}$ is used in Eq. (8) to update each element of the thermal dose vector ***TD*** corresponding to tanks in the "*vulnerable*" status:

$$TD_i(ttf_{MVT}) = TD_i(t) + \int_t^{ttf_{MVT}} TR_i^{\alpha} \cdot d\tau \tag{8}$$

where $TD_i\ (ttf_{MVT})$ and $TD_i\ (t)$ are respectively the updated and the previous value of the thermal dose for the *i-th* target, $TR_i$ is the thermal radiation received by the *i-th* tank in the time interval between $t$ and $ttf_{MVT}$, and $\alpha$ is a constant (as defined in Section 2.2.2). Once the thermal dose vector is updated, the time $t$ is updated as well, setting it equal to $ttf_{MVT}$.

### 2.2.5. Development of sub-branches

The lower sub-branch (see Fig. 3) takes into account the case in which the most vulnerable target does not fail, i.e., the case in which the intervention of emergency teams is effective. Thus, the element of the status vector related to the *MVT* should be set to "*protected*".

Contrarily, the upper sub-branch (see Fig. 3) considers the case in which the intervention of the emergency teams is not effective, and a failure of the *MVT* occurs. Thus, the consequences related to *MVT* failure should be assessed. This is done applying the well-established literature models for the calculation of pool fire thermal radiation following atmospheric tank failure [79,86,87]. Given the failure of the *MVT*, the possibility of escalation to other equipment items due to thermal radiation should be considered. If the escalation is not possible (i.e., the final outcome of the *MVT* does not lead to a stationary fire scenario), the status of the MVT is set to "*failed*". Otherwise, the status is set to "*on fire*". In all cases, a new iteration of the procedure is performed if other targets in "*vulnerable*" status are present.

### 2.2.6. Branch probability calculation and event tree completion

When no more targets in "*vulnerable*" status are present in a branch, the probability of occurrence of the given *k-th* branch $P_k$ can be assessed according to Eq. (9):

$$P_k = \prod_{i=1}^{n_T} \left(1 - p_{f,i,k} + \beta_{i,k} \cdot \left(2 \cdot p_{f,i,k} - 1\right)\right) \tag{9}$$

where $p_{f,i,k}$ is the failure probability of the *i-th* target in the *k-th* branch calculated according to Section 2.2.3 and $\beta_{i,k}$ is a factor equal to 0 when the status of the *i-th* target in the *k-th* branch is "*protected*", 1 otherwise. Clearly, each branch derived from the procedure represents a combined scenario in which a given number of tanks fail. Once the calculation of the probability of occurrence of a branch is completed, the procedure continues analyzing other branches. When the analysis of all branches is completed, the procedure ends.

**Table 1**
Modification considered for the parameters used in the calculation of the probit variable in Eq. (7) in order to take into account harsh environmental conditions generated by the wildfire.

| Parameters | $\gamma = 1$ | $\gamma = 2$ |
|---|---|---|
| Lower reference value for the intervention time [min] | 5 | 10 |
| Upper reference value for the intervention time [min] | 20 | 40 |
| Coefficient A in Eq. (7) | 9.257 | 10.539 |
| Coefficient B in Eq. (7) | -1.849 | -1.849 |

### 2.3. Vulnerability and risk assessment

#### 2.3.1. Vulnerability assessment

Once all possible scenarios are generated, the assessment of the consequence of the overall scenarios is performed (Step 3.1 in Fig. 1). The overall death probability of each *k-th* combined scenario is calculated applying the approach proposed by Cozzani and co-workers [46–48,88–90]:

$$C_k = \min\left(\sum_{i=1}^{n_T} \delta_i \cdot C_i, 1\right) \tag{10}$$

where $C_k$ is the death probability in the position of interest calculated for the overall scenario *k*, $C_i$ is the death probability in the same position associated with the *i-th* equipment item, and $\delta_i$ assumes a value of 1 if the corresponding fire is ongoing, 0 otherwise. The death probability related to each failed piece of equipment, $C_i$, can be estimated by applying a human vulnerability model to the radiation intensity [79,91]. In the present approach, the probit model for fatalities caused by radiation reported in the TNO green book [92] was used.

Three vulnerability indexes were defined and assessed to support the analysis of results (Step 3.2 in Fig. 1). The first is the overall failure probability $P_{f,i}$ of the *i-th* tank considering all the branches in which the item fails, calculated according to Eq. (11):

$$P_{f,i} = \sum_{k=1}^{n_k} P_k \cdot \beta_{i,k} \tag{11}$$

where $P_k$ is the probability of occurrence of the *k-th* branch calculated according to Eq. (9) and $\beta_{i,k}$ is a factor equal to 0 when the status of the *i-th* target in the *k-th* branch is "*protected*", 1 otherwise.

The second index (Synergistic Effect Index $SEI_i$) accounts for the increase in the failure probability of the *i-th* tank due to the synergistic effect of the wildfire and the domino effect together compared to considering the two triggers separately, and it is evaluated as follows:

$$SEI_i = \frac{P_{f,i} - \max\left(P_{f,i}^{wf}, P_{f,i}^{de}\right)}{P_{f,i}} \tag{12}$$

where $P_{f,i}$ is the overall failure probability of the *i-th* tank calculated applying the methodology developed in the present study, $P_{f,i}^{wf}$ is the overall failure probability of the *i-th* tank considering the wildfire only, and $P_{f,i}^{de}$ is the overall failure probability of the *i-th* tank considering the domino effect only.

The last one (Hazard Index $HI_i$) represents the relevance of the *i-th* tank on the overall consequences. The unit hazard index $UHI_i$ is calculated as the product of the overall failure probability $P_{f,i}$ of the *i-th* tank and the related damage distance $d_i$. The layout hazard index *LHI* is defined as the sum of the $UHI_i$ of all the tanks present in the layout. Eventually, the Hazard Index of the *i-th* tank is calculated as a function of the layout hazard index considering the exclusion of the *i-th* tank as follows:

$$HI_i = \frac{LHI - LHI_i}{LHI} \tag{13}$$

where *LHI* is the layout hazard index of the entire configuration, and $LHI_i$ represents the layout hazard index excluding the *i-th* tank. Noteworthy, the overall failure probability of each tank remaining in the layout should be updated accordingly. A threshold value of 7 kW/m$^2$ was considered in the calculation of the damage distances accounting for effects on humans, as widely adopted in the literature [93–95].

Besides the calculation of vulnerability indexes, the extension of zones potentially affected by the wildfire events may be determined by calculating "lethality maps". Lethality maps are contour plots in which curves related to a given death probability are reported. These maps allow the identification of the areas of the site most affected by technological scenarios triggered by wildfire events. Given the similarities in the physical effects on human health, the contribution of wildfire is also considered. The value of the lethality *L* (overall death probability in a given position at a given time) is calculated considering the death probability deriving from each scenario ($C_k$) and the conditional probability of the scenario given the wildfire ($P_k$):

$$L = \sum_{k=1}^{n_k} P_k \cdot C_k \tag{14}$$

#### 2.3.2. Risk assessment

Vulnerability indexes may be used to calculate individual and societal risk maps (Step 3.3 of the methodology, see Fig. 1). As discussed above, the detailed modeling of wildfires is out of the scope of the present approach. However, it should be highlighted that a few methodologies are available in the literature for the quantitative assessment of the likelihood of wildfires (e.g., see Gao et al. [96]; Guyette et al. [97]; Thompson et al. [98]). Thus, starting from the output of such models it is possible to combine wildfire expected frequencies to lethality maps to obtain specific risk figures: the location-specific individual risk (LSIR) and the societal risk. The LSIR maps provide the probability of death of unprotected individuals exposed to the risk in each position of the site of concern, thus it allows identifying the more critical areas in the site [99]. If the distribution of workers and resident population before or after evacuation is known, the cumulative frequency (F) versus the overall number of fatalities (N) F/N societal risk curve may be calculated as well [79,91,99], together with other indices supporting a more concise presentation of societal risk figures such as the Potential Life Loss (PLL) [88–90,100–102]:

$$PLL = \sum_{N} f(N) \cdot N \tag{15}$$

## 3. Case Study

A case study was defined to demonstrate the application of the proposed methodology and the results that may be obtained. The case study consists of a storage area where 17 atmospheric tanks are present. The main features of the equipment items are reported in Table 2. The layout considered in the case study is shown in Fig. 4.

A forest faces the northern border of the storage site (green area in Fig. 4). The average height of vegetation $H_v$ is assumed to be equal to 10 m. Distances between the vegetation and each tank $D_v$ are reported in Table 3. The table also reports the separation distances (center to edge) among tanks.

The simplified approach suggested in Section 2.1.1 was applied to obtain a preliminary characterization of the wildfire. Thus, the wildfire is modeled as reported in Fig. 2, and the following input parameters were considered for the wildfire: a flame black body temperature of 1200 K, a flame length equal to 3.5 times the height of the vegetation (i.e., 35 m), an infinite value of the fire-front width, the flame tilt angle θ that maximizes the incident radiation based on the separation distance

**Table 2**
Features of the equipment items considered in the case study.

| Parameters | T1-T3, T12-T17 | T4-T8 | T9-T11 |
|---|---|---|---|
| Type | Atmospheric tank | Atmospheric tank | Atmospheric tank |
| Nominal volume [m$^3$] | 9975 | 9161 | 12367 |
| Diameter [m] | 42 | 36 | 54 |
| Height [m] | 7.2 | 9 | 5.4 |
| Filling level [-] | 0.75 | 0.75 | 0.75 |
| Substance | Gasoline | Gasoline | Crude oil |
| Physical state | Liquid | Liquid | Liquid |
| Operating pressure [bar] | 1.01 | 1.01 | 1.01 |
| Inventory [ton] | 5612 | 5153 | 8812 |

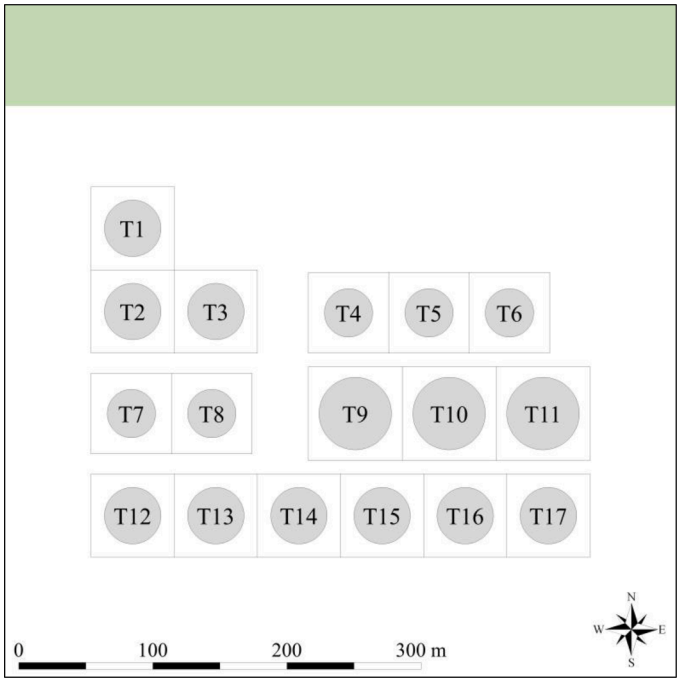


**Fig. 4.** Layout considered in the case study. The green area in the figure represents the forest front.

from vegetation and tanks, and a maximum duration of the wildfire scenario equal to 15 min.

It is important to remark that the case study complies with the safety distances from vegetation prescribed by the Health and Safety Executive [43] and by other national regulations [40–42,44]. However, tanks T1 to T6 have distances lower than the conservative safety distances *SD* specific for wildfires suggested by Ricci et al. [45] and reported in Table 3. Differently, tanks from T7 to T17 have a distance from the vegetation higher than the specific conservative values calculated by the approach of Ricci et al. [45]. Thus, the integrity of these items cannot be compromised considering only the wildfire event, since their time to failure is higher than the maximum duration of the wildfire. Thus, possible failure in the case of a wildfire scenario is only due to domino effects from nearby tanks.

Given the features of the tanks present in the layout of the case study and the flammable substances contained, the catastrophic rupture of the target followed by an immediate ignition leading to a pool fire is considered in the analysis. Well-established literature models were applied to perform the consequence analysis of each scenario [79,86,87]. For the sake of simplicity, a single set of meteorological conditions was considered in the analysis of the case study: a uniform wind distribution and neutral atmospheric stability (wind speed at 5 m/s, Pasquill class D) [86,99].

Fig. 5 reports the consequence assessment for the three types of tanks present in the layout (i.e., the incident radiation from the pool fire center as a function of the distance). The figure also reports the incident radiation from the wildfire calculated according to Eq. (2). Based on the distances reported in Table 3 and on the consequence assessment of each scenario present in Fig. 5, the incident radiation received by each tank is calculated.

The dynamic approach introduced in the present study is evaluated with respect to conventional static methodologies proposed in the literature for the evaluation of Natech scenarios and domino effects [46–48,90]. The importance of delays in the deployment of mitigation actions is also assessed. The comparison was carried out considering the following cases:

- **Case 0** (Conventional methodology with reference intervention times). The assessment is performed according to the original methodology proposed by Cozzani et al. [46] assuming 5 and 20 min as the lower and upper values for the intervention time (i.e., $\gamma = 1$, in Table 1)
- **Case 1** (Present methodology with reference intervention times). The assessment is performed according to the dynamic methodology developed in the present study assuming $\gamma = 1$ in Table 1.
- **Case 2** (Present methodology with delayed intervention times). The evaluation is performed according to the dynamic methodology developed in the present study considering a delay in the emergency intervention. A delay factor $\gamma$ equal to 2 is assumed to evaluate the probit variable (see Section 2.2.3 and Table 1).

In order to provide a more complete demonstration of the potential application of the methodology, individual and societal risk indexes were calculated for the case-study. A realistic value for the time of return of wildfires was used in the assessment of the case study, derived from the data obtained by Guyette et al. [97] for the Willamette Valley site (Oregon, USA). The predicted Mean Fire Interval in the area is around 6 years. Thus, a wildfire frequency $f_{wf}$ of $1.67 \bullet 10^{-1}$ was assumed. A uniform population density of 100 people/ha and a presence probability of 60 % were assumed for societal risk calculations.

**Table 3**
Distances (in meters) of each tank from the vegetation ($D_v$) and the other tanks in the layout considered (see Fig. 4). Distances are calculated from the center of the tank considered to the edge of receptors. Specific safety distances calculated according to Ricci et al. [45] are also reported (*SD*).

| $T_i \backslash T_j$ | $D_v$ | SD | T1 | T2 | T3 | T4 | T5 | T6 | T7 | T8 | T9 | T10 | T11 | T12 | T13 | T14 | T15 | T16 | T17 |
|---|---|---|---|---|---|---|---|---|---|---|---|---|---|---|---|---|---|---|---|
| T1 | 70 | 169 | - | 41 | 67 | 152 | 209 | 267 | 117 | 129 | 195 | 253 | 315 | 193 | 202 | 227 | 263 | 307 | 356 |
| T2 | 132 | 169 | 41 | - | 41 | 140 | 200 | 260 | 55 | 75 | 162 | 227 | 295 | 131 | 143 | 175 | 219 | 270 | 325 |
| T3 | 132 | 169 | 67 | 41 | - | 78 | 138 | 198 | 78 | 55 | 108 | 169 | 235 | 143 | 131 | 143 | 175 | 219 | 270 |
| T4 | 136 | 166 | 155 | 143 | 81 | - | 42 | 102 | 161 | 109 | 57 | 88 | 145 | 203 | 163 | 138 | 135 | 157 | 194 |
| T5 | 136 | 166 | 212 | 203 | 141 | 42 | - | 42 | 217 | 161 | 75 | 59 | 96 | 250 | 202 | 162 | 137 | 136 | 158 |
| T6 | 136 | 166 | 270 | 263 | 201 | 102 | 42 | - | 274 | 217 | 120 | 70 | 61 | 301 | 248 | 200 | 161 | 137 | 136 |
| T7 | 211 | 166 | 120 | 58 | 81 | 161 | 217 | 274 | - | 42 | 149 | 219 | 289 | 58 | 81 | 129 | 184 | 243 | 302 |
| T8 | 211 | 166 | 132 | 78 | 58 | 109 | 161 | 217 | 42 | - | 89 | 159 | 229 | 78 | 58 | 82 | 130 | 186 | 245 |
| T9 | 202 | 179 | 189 | 156 | 102 | 48 | 66 | 111 | 140 | 80 | - | 43 | 113 | 156 | 102 | 60 | 52 | 85 | 136 |
| T10 | 202 | 179 | 247 | 221 | 163 | 79 | 50 | 61 | 210 | 150 | 43 | - | 43 | 221 | 163 | 109 | 64 | 50 | 79 |
| T11 | 202 | 179 | 309 | 289 | 229 | 136 | 87 | 52 | 280 | 220 | 113 | 43 | - | 289 | 229 | 170 | 115 | 69 | 49 |
| T12 | 284 | 169 | 193 | 131 | 143 | 200 | 247 | 298 | 55 | 75 | 162 | 227 | 295 | - | 41 | 103 | 165 | 227 | 289 |
| T13 | 284 | 169 | 202 | 143 | 131 | 160 | 199 | 245 | 78 | 55 | 108 | 169 | 235 | 41 | - | 41 | 103 | 165 | 227 |
| T14 | 284 | 169 | 227 | 175 | 143 | 135 | 159 | 197 | 126 | 79 | 66 | 115 | 176 | 103 | 41 | - | 41 | 103 | 165 |
| T15 | 284 | 169 | 263 | 219 | 175 | 132 | 134 | 158 | 181 | 127 | 58 | 70 | 121 | 165 | 103 | 41 | - | 41 | 103 |
| T16 | 284 | 169 | 307 | 270 | 219 | 154 | 133 | 134 | 240 | 183 | 91 | 56 | 75 | 227 | 165 | 103 | 41 | - | 41 |
| T17 | 284 | 169 | 356 | 325 | 270 | 191 | 155 | 133 | 299 | 242 | 142 | 85 | 55 | 289 | 227 | 165 | 103 | 41 | - |

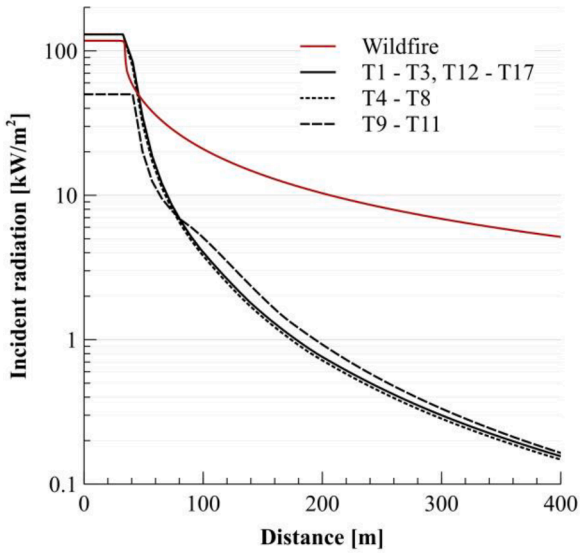


**Fig. 5.** Incident radiation vs. distance from the wildfire and from the pool fires following tank failure. Distances are calculated from the center of the pool fires and from the edge of the vegetation (see Fig. 4).

## 4. Results

### 4.1. Application of the developed methodology

The case study defined in Section 3 was used to demonstrate the applicability of the methodology and to highlight the results that can be obtained from its implementation.

Table 4 shows the main results obtained from the first iteration of the methodology, where the only source of thermal radiation is the wildfire. In the case of tanks where the duration of the wildfire is lower than the *ttf*, two values of the thermal radiation are reported in the table (during and after the wildfire).

As shown in Table 4, T1 was identified as the most vulnerable tank (*MVT*), since it features the lowest *ttf* among all the targets considered. The failure probability ($p_f$) of T1 was calculated by the methodology defined in Section 2.2.3 and resulted equal to 0.881. The thermal dose received by the other targets ($TD_i$) was then updated as indicated in Fig. 3. Clearly, the thermal dose of T1 is equal to its critical value ($TD_C$).

Then, the time $t$ is set equals to the *ttf* value of the most vulnerable target (i.e., T1 with $ttf = 316.8$ s), and two branches are introduced in the event tree: the lower branch considers the case in which the tank is successfully protected, while the upper branch considers its failure. Since the ***S*** vector contains other elements in "*vulnerable*" status, the procedure continues with a new iteration, as described in Section 2.2.5. Table 5 reports the features of the ***S*** and ***TR*** vectors updated at time 316.8 s ($ttf_{MVT}$) in the lower and upper branches of the event tree. As shown in the table, in the lower branch, assuming the successful mitigation of the *MVT*, no update of the intensity of the thermal radiation values ($TR_i$) is required since the wildfire remains the only radiation source. Differently, in the upper branch of the event tree, the ***TR*** vector is updated to account for the fire at tank T1. Noteworthy, the end of the wildfire after 15 min is considered in the time to failure calculation. In addition, the $ttf_i$ of each tank in the vulnerable state is reported in Table 5, and T2 is identified as the new *MVT* in both branches. Nevertheless, tank T2 features different time to failure in the two branches, and therefore failure probabilities also change, being respectively 0.826 in the upper branch and 0.423 in the lower one. After the selection of the *MVT*, the ***TD*** vector is updated, and the time $t$ is set equal to $ttf_{MVT}$ of the related branch.

Applying iteratively the procedure reported in Fig. 3 and described in Section 2.2, all the possible scenarios arising from the wildfire are thus defined and quantified.

**Table 4**
Main outcomes of the first iteration of the dynamic methodology. The most vulnerable target is reported in italic. $TR_i$: thermal radiation received by the *i-th* target, $ttf_i$: time to failure of the *i-th* target; $TD_i$: thermal dose of the *i-th* target updated at the time to failure of the *MVT*.

| Tank ID | *S* vector | $TR_i$ [kW/m$^2$] | $ttf_i$ [s] | $TD_i$ [kJ/m$^2$] |
|---|---|---|---|---|
| *T1* | *Vulnerable* | *30.4* | 316.8 | *14928* |
| T2 | Vulnerable | 15.7 | 666.7 | 7094 |
| T3 | Vulnerable | 15.7 | 666.9 | 7091 |
| T4 | Vulnerable | 15.3 | 705.1 | 6855 |
| T5 | Vulnerable | 15.3 | 704.8 | 6858 |
| T6 | Vulnerable | 15.3 | 704.5 | 6860 |
| T7 | Vulnerable | 9.8 – 0 | > 900 | 4151 |
| T8 | Vulnerable | 9.8 – 0 | > 900 | 4151 |
| T9 | Vulnerable | 10.2 – 0 | > 900 | 4362 |
| T10 | Vulnerable | 10.2 – 0 | > 900 | 4362 |
| T11 | Vulnerable | 10.2 – 0 | > 900 | 4362 |
| T12 | Vulnerable | 7.3 – 0 | > 900 | 2964 |
| T13 | Vulnerable | 7.3 – 0 | > 900 | 2964 |
| T14 | Vulnerable | 7.3 – 0 | > 900 | 2964 |
| T15 | Vulnerable | 7.3 – 0 | > 900 | 2964 |
| T16 | Vulnerable | 7.3 – 0 | > 900 | 2964 |
| T17 | Vulnerable | 7.3 – 0 | > 900 | 2964 |

### 4.2. Failure probability of equipment items

The dynamic methodology developed in the present study was compared to the static conventional methodology developed by Cozzani et al. [46] for the quantitative risk assessment of Natech accidents and

**Table 5**
Updated values of the *S*, *TR*, and *TD* vectors and $ttf_i$ for the upper and lower branches of the event tree after time 316.8 s, corresponding to *ttf* of tank T1. The most vulnerable target is reported in italic.

| Tank ID | S vector | $TR_i$ [kW/m$^2$] | $ttf_i$ [s] | $TD_i$ [kJ/m$^2$] |
|---|---|---|---|---|
| ***Upper branch*** | | | | |
| T1 | On fire | 30.4 | 316.8 | 14928 |
| *T2* | *Vulnerable* | *98.8* | *360.9* | *14928* |
| T3 | Vulnerable | 27.3 | 504.6 | 8929 |
| T4 | Vulnerable | 16.7 | 668.5 | 7907 |
| T5 | Vulnerable | 15.9 | 686.6 | 7858 |
| T6 | Vulnerable | 15.7 | 693.8 | 7841 |
| T7 | Vulnerable | 12.4 – 2.6 | 1266 | 4907 |
| T8 | Vulnerable | 11.9 – 2.1 | 1601 | 4869 |
| T9 | Vulnerable | 11.1 – 0.9 | 1891 | 5027 |
| T10 | Vulnerable | 10.7 – 0.5 | 3683 | 5000 |
| T11 | Vulnerable | 10.5 – 0.3 | 6603 | 4987 |
| T12 | Vulnerable | 8.1 – 0.8 | 8112 | 3429 |
| T13 | Vulnerable | 8 – 0.7 | 9106 | 3424 |
| T14 | Vulnerable | 7.8 – 0.6 | 12161 | 3413 |
| T15 | Vulnerable | 7.7 – 0.4 | 17825 | 3402 |
| T16 | Vulnerable | 7.5 – 0.3 | 26653 | 3394 |
| T17 | Vulnerable | 7.5 – 0.2 | 38984 | 3389 |
| ***Lower branch*** | | | | |
| T1 | Protected | 30.4 | 316.8 | 14928 |
| *T2* | *Vulnerable* | *15.7* | *666.7* | *14928* |
| T3 | Vulnerable | 15.7 | 666.9 | 14922 |
| T4 | Vulnerable | 15.3 | 705.1 | 14425 |
| T5 | Vulnerable | 15.3 | 704.8 | 14431 |
| T6 | Vulnerable | 15.3 | 704.5 | 14437 |
| T7 | Vulnerable | 9.8 – 0 | > 900 | 8736 |
| T8 | Vulnerable | 9.8 – 0 | > 900 | 8736 |
| T9 | Vulnerable | 10.2 – 0 | > 900 | 9179 |
| T10 | Vulnerable | 10.2 – 0 | > 900 | 9179 |
| T11 | Vulnerable | 10.2 – 0 | > 900 | 9179 |
| T12 | Vulnerable | 7.3 – 0 | > 900 | 6237 |
| T13 | Vulnerable | 7.3 – 0 | > 900 | 6237 |
| T14 | Vulnerable | 7.3 – 0 | > 900 | 6237 |
| T15 | Vulnerable | 7.3 – 0 | > 900 | 6237 |
| T16 | Vulnerable | 7.3 – 0 | > 900 | 6237 |
| T17 | Vulnerable | 7.3 – 0 | > 900 | 6237 |

Domino events. Fig. 6 reports the overall failure probability of each tank present in the layout $P_{f,i}$ (panel a) and the probability of simultaneous failure of a given number of items (panel b) according to the three cases defined in Section 3. A higher $P_{f,i}$ is calculated by the static methodology (Case 0 in Fig. 6-a) than the dynamic methodology (Case 1 in Fig. 6-a) for tanks that can fail due to the wildfire only (T1 to T6) when the same intervention time is accounted for the emergency teams. Nevertheless, according to the dynamic methodology, a higher number of tanks may be involved in the scenario. Indeed, tanks T12 to T17 may be affected by the domino effect. On the contrary, these tanks are not involved in the cascading sequence when the static methodology is considered, since in the latter only first-order domino effects are considered [46]. Thus, the simultaneous failure of up to 11 tanks is credible according to the static methodology (Case 0 in Fig. 6-b), while the dynamic one attributes a non-negligible probability to the failure of all the equipment items present in the layout (Case 1 in Fig. 6-b). Overall, Fig. 6 confirms that in Case 0 the possibility of simultaneous scenarios triggered by the wildfire is underestimated since the dynamic behavior of the scenario leading to higher-order domino effects is not considered.

Not surprisingly, the overall failure probability of each tank increases when considering a higher intervention time of the emergency teams (see the comparison of Case 1 and Case 2 in Fig. 6-a). It is worth mentioning that, when considering the simultaneous failure of equipment items, the scenario having the highest probability considers the simultaneous failure of 8 tanks in the case of standard intervention times (Case 1 in Fig. 6-b). Differently, the scenario having the highest probability when delays related to emergency teams are taken into account (Case 2 in Fig. 6-b) considers the simultaneous failure of 16 tanks. Moreover, besides the increase in the number of equipment items involved, the maximum probability of the scenario is also higher, resulting in more than doubled in the case of delayed intervention times.

### 4.3. Sensitivity analysis

Fig. 7 shows the results of a sensitivity analysis carried out to evaluate the influence of the input parameters used for wildfire characterization on the overall failure probability of tanks. The three main parameters defining a wildfire were included in the analysis: the flame black body temperature, the maximum exposure time to wildfire, and the flame length. A variation of the 10% of each parameter was considered starting from the values used in the case-study (i.e., $T_f$ = 1200 K, $t_{wf}$ = 900 s, and $L_f = 3.5 \bullet H_v$). The standard intervention time of emergency response is considered in the sensitivity analysis (see γ=1 in Table 1 for more details).

It is clear from Fig. 7 that the flame black body temperature is the parameter that mostly influences the results, causing a variation in the overall failure probability of about an order of magnitude. It should be remarked that the variation in the flame blackbody temperature leads to a modification of the thermal radiation reaching tanks and therefore of the time to failure of tanks. As a consequence, equipment items whose failure can be directly caused by wildfire events depend on the temperature assumed.

The effect of the flame length is much lower than that of the flame black body temperature. Indeed, an average variation of about 30% in the overall failure probability of each tank was obtained when considering a flame length variation of 10% (see Fig. 7b).

The maximum exposure time to the wildfire has the lowest influence on the overall failure probability, as reported in Fig. 7c. The average modification of $P_{f,i}$ is lower than 3% when considering the exposure time.

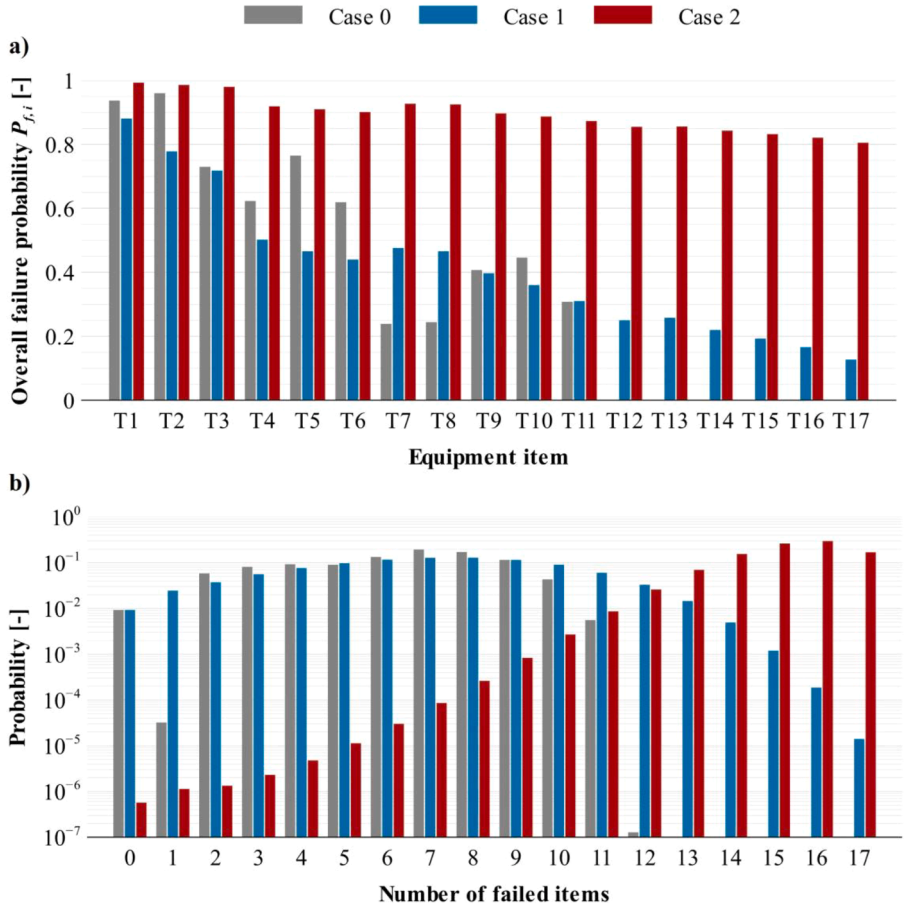


**Fig. 6.** Overall failure probability of each tank (a) and probability of simultaneous failure of a given number of items (b) for the three cases defined in Section 3.

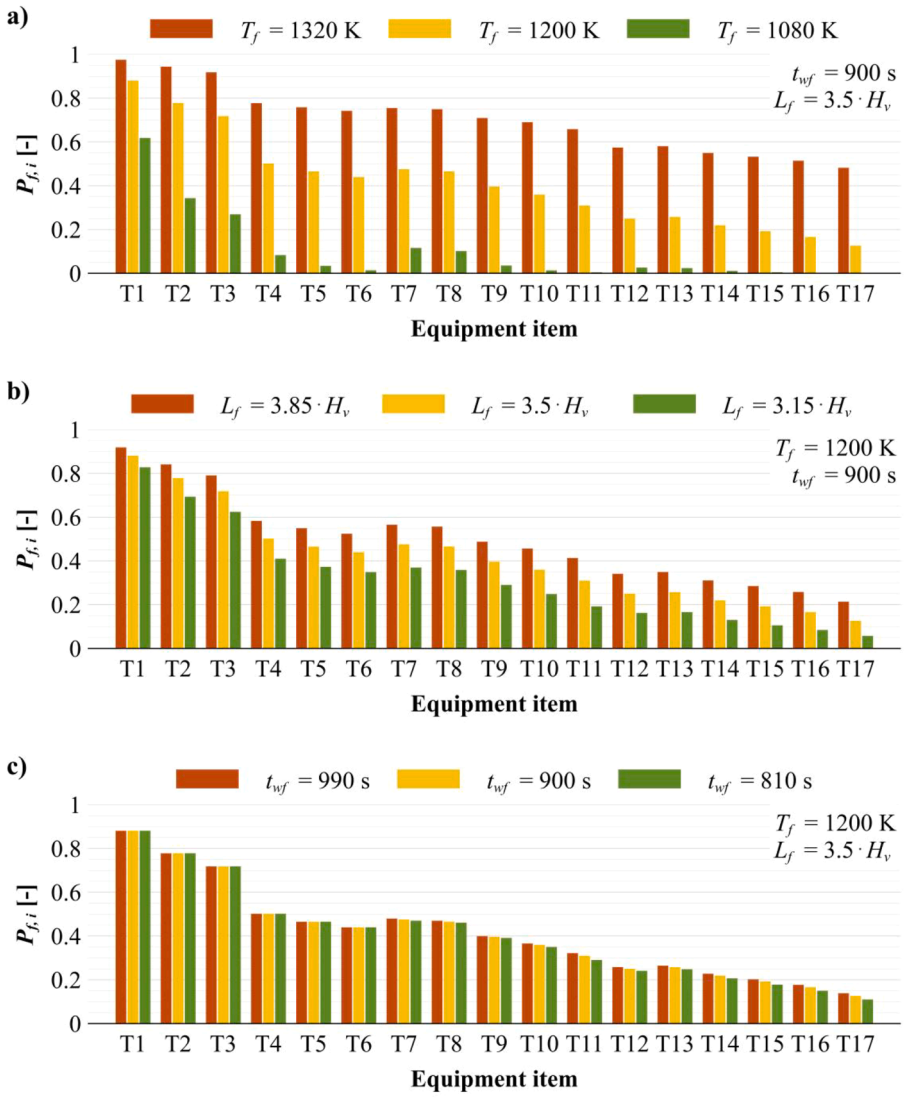


**Fig. 7.** Results of the sensitivity analysis for the overall failure probabilities of tanks $P_{f,i}$ considering a variation of the 10% on (a) flame black body temperature $T_f$, (b) flame length $L_f$, and (c) maximum exposure time to wildfire $t_{wf}$.

It is worth remarking that for all the three parameters considered, the higher modifications occur for the tanks that are more far away from the fire front, and in particular for those whose failure may only be caused by domino effects.

### 4.4. Vulnerability indexes

Fig. 8 reports the results obtained for the vulnerability indexes calculated for the case study: the Synergistic Effect Index, $SEI_i$, and the Hazard Index, $HI_i$ (see Section 2.3). The $SEI_i$ accounts for the increase in the overall failure probability of each tank due to the synergistic effects of multiple simultaneous fires. The $HI_i$ provides a preliminary assessment of the relevance of the consequence of the failure of each tank on the overall consequences of the fire scenario. Both indexes were calculated for each tank applying the dynamic methodology (Case 1).

According to Fig. 8-a, the synergistic effect introduced in the present methodology has a low relevance for tanks that may fail due to the wildfire only (T1 to T6). On the contrary, the increase in the overall failure probability for the other tanks is relevant, up to a value near 1 for those far from the wildfire. Thus, these tanks would have an almost zero chance of failure due to the wildfire or domino effect alone, synergic effects being the main responsible for tank failure. Hence, neglecting the synergic effects would lead to a relevant underestimation of the vulnerability.

The Hazard Index $HI_i$ (Fig. 8-b) takes into account both the overall failure probability $P_{f,i}$ and the damage distance $d_i$ of each tank. Thus, the higher the value of $HI_i$, the higher the relevance of the *i-th* tank on the overall consequences. As can be seen in the figure, tanks featuring a high $SEI_i$ are those with a lower value of the $HI_i$. Clearly, such tanks are those that fail at the end of the accident chain, thus providing a lower contribution to the escalation of the accident. Conversely, the tanks that typically fail early in the accidental chain (for example T1 and T2, as reported in Table 4 and Table 5) are those with a high value of $HI_i$.

The $HI_i$ provides useful indications to support decision-making concerning the implementation of safety barriers. Indeed, protecting the tanks with the highest Hazard Index (and therefore excluding them from the accident chain) results in relevant mitigation of the overall consequences of the accident scenario.

In Fig. 9, the lethality maps for the case study defined in Section 3 are reported. Lethality maps show the probability of death of an unprotected individual as a function of the position in the area of interest, given the initiating event (i.e., the wildfire). The figure reports the maps obtained considering only the wildfire (Fig. 9-a) and those including primary Natech and domino effect scenarios. These were considered both

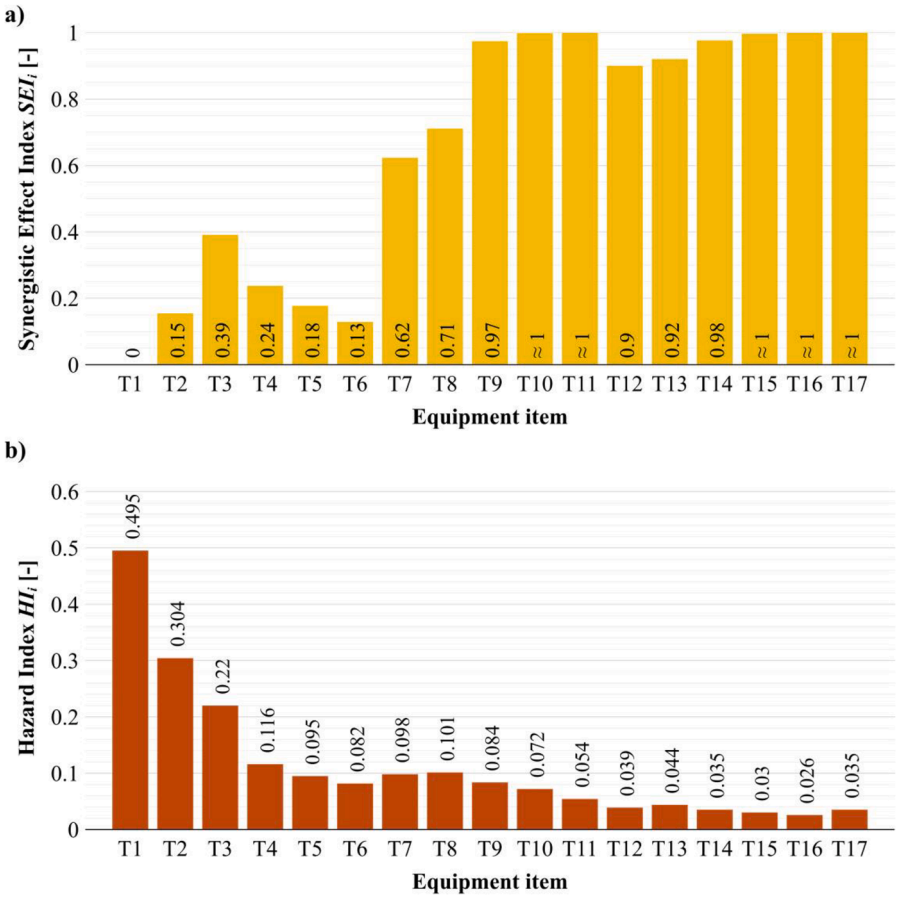


**Fig. 8.** Synergistic Effect Index (a) and Hazard Index (b) related to Case 1.

applying the static methodology (Case 0, Fig. 9-b) and the dynamic approach developed in the present study, considering different intervention times (Case 1, Fig. 9-c, and Case 2, Fig. 9-d). As shown in the figure, the extension of the areas where the death probability is higher than 0.1 increases considerably when including the primary Natech scenario and the related domino effects. According to the dynamic methodology developed in the present study and considering standard intervention times (Case 1, Fig. 9-c), the area where the death probability is higher than 0.1 (10 %) extends to a distance up to 350 m from the vegetation, around 3 times higher than the distance calculated considering only the wildfire. When considering a delay in the intervention time (Case 2, Fig. 9-d), the affected area is similar, but the death probability within the area is higher. Indeed, the area where the death probability is higher than 0.9 is approximately 1.6 times larger than that calculated considering standard intervention times. Remarkably, the area calculated applying the static methodology (Case 0, Fig. 9-b) is lower than that obtained from the dynamic methodology. Indeed, as observed in Fig. 6, tanks from T12 to T17 are not considered to be involved in the accident chain when applying the static methodology.

### 4.5. Risk indexes

As discussed above, the vulnerability results may be used to calculate individual and societal risk indexes when of interest. Fig. 10 reports the Local-Specific Individual Risk plots obtained for the case-study. As shown in the figure, even if the overall extension of the affected area is almost the same for both the standard (Case 1, Fig. 10-a) and delayed intervention time (Case 2, Fig. 10-b), the values of LSIR increase considerably when the emergency teams intervention is delayed.

Fig. 11 reports the PLL values calculated for all the cases defined in Section 3. It can be noted how the PLL value obtained from the dynamic approach proposed in this study (43 1/y) is higher than the one calculated with the static methodology available in the literature (37 1/y). The increase in the PLL becomes more evident when a delay in the intervention time is considered (87 1/y), confirming the relevance of the intervention time on risk figures.

## 5. Discussion

An innovative approach was obtained for the dynamic vulnerability assessment of industrial tank farms exposed to wildfires. The methodology accounts for both the primary Natech scenarios and the possible escalation caused by domino effects triggered by fires. A dynamic event tree is introduced to identify the chains of failures considered. Each chain accounts for the failure of tanks based on their time to failure (*ttf*) in a given fire scenario. First-order and higher-order domino effects are considered in the developed approach. The developed procedure considers the time dependence of the events, which was disregarded in previous methodologies for Natech vulnerability and risk assessment. Thus, the methodology is able to capture the dynamic features of the scenario resulting from the wildfire and the synergistic effect of the cascading technological scenarios are taken into account. The analysis of a case study evidenced that neglecting the dynamic features of wildfire and related technological cascading events may lead to an underestimation of the actual vulnerability of tank farms to Natech events triggered by wildfires and interface fires.

The results obtained also show the importance of the intervention time on the vulnerability. This confirms the results reported in recent studies that identified the possible depletion of safety barriers as one of the most critical aspects in Natech accidents [103–105], since natural

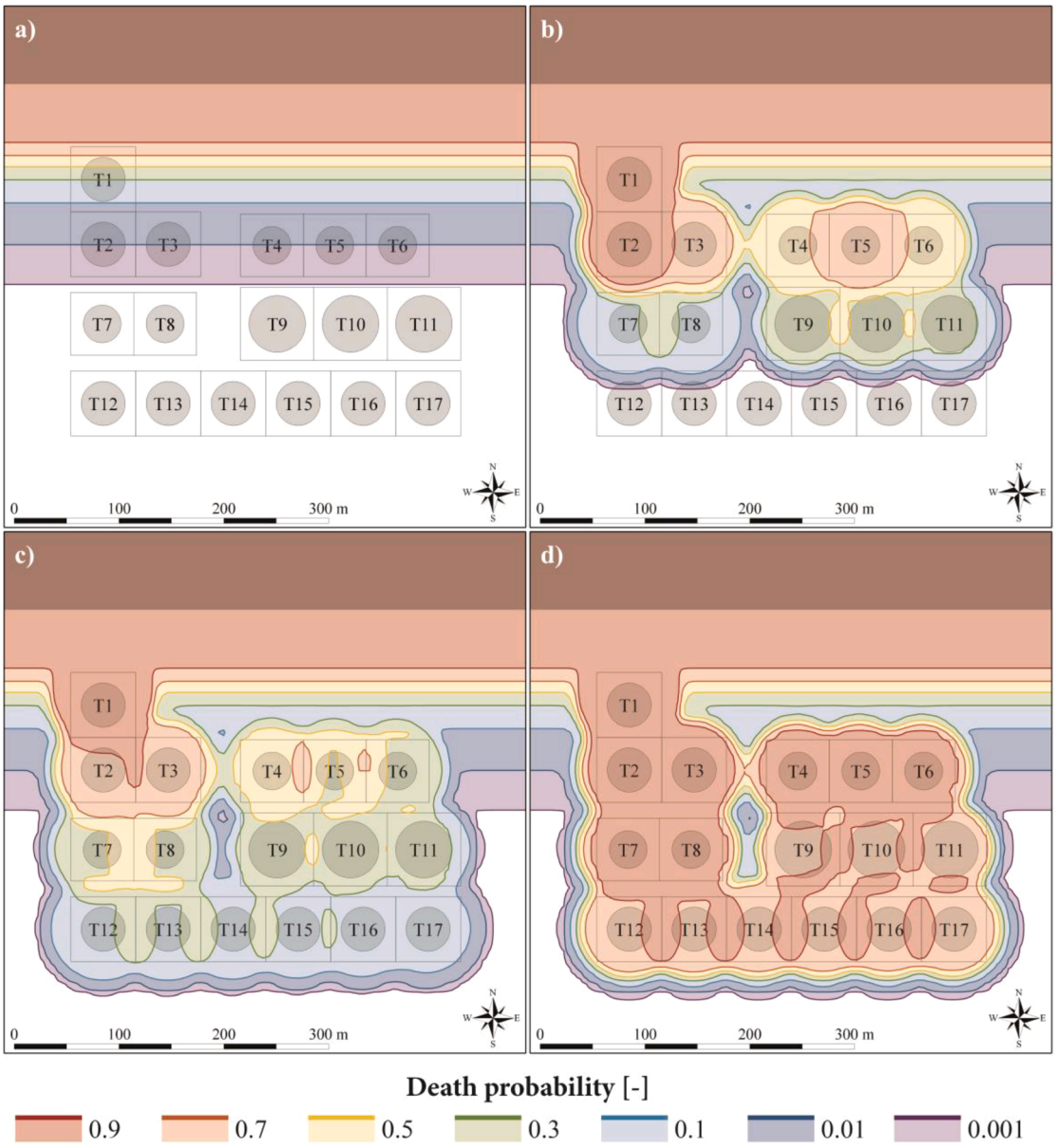


**Fig. 9.** Lethality maps reporting the death probability calculated given the initiating event. (a) wildfire only; (b) wildfire + Case 0; (c) wildfire + Case 1; (d) wildfire + Case 2.

events may hamper and delay the emergency response [106–109]. As shown in Fig. 10 and Fig. 11, this may result in a relevant increase in risk (up to a factor 2 for the case study considered). Hence, an accurate evaluation of the intervention time is paramount to properly quantify the vulnerability and risk. It should be remarked that the emergency intervention times used in the assessment of the case study have a purely illustrative purpose. In perspective, addressing the detailed assessment of the time required for the emergency response is crucial to obtain more accurate vulnerability and risk figures when assessing cascading sequences in Natech scenarios [8,106,109,110].

The case study evidences the relevant vulnerability of tank farms to wildfires. As shown in Figs. 7 and 9, the failure probability of the tanks considered is high and the lethality obtained in the proximity of the tank farm reaches values up to above 0.9. These figures are of particular concern from the perspective of climate change, which increases the likelihood of severe interface fires and wildfires affecting the vegetation in the vicinity of industrial sites. Thus, appropriate management of clearance areas and the revisitation of safety distances for vulnerable elements are key issues to provide adequate protection of industrial sites from this type of hazard. In this framework, the Hazard Index defined in the present study may support decision-making concerning the application of safety barriers for the protection of critical equipment items.

Although the present version of the methodology is only suitable to consider escalation caused by thermal radiation, due to the specific calculation pattern adopted in the generation of the scenarios, the overall approach may be used to address the vulnerability of more complex Natech scenarios. In perspective, the methodology can be extended to include other scenarios which may lead to escalation vectors such as blast waves and missiles.

A final remark concerns the risk indexes that may be obtained from the vulnerability maps. Clearly enough, risk figures are relevant only if workers or the population are not evacuated from the site. Actually, evacuation procedures, especially in interface fires, may not be always effective. For instance, during the Black Saturday brushfires in Victoria (Australia, 2009), 35 out of the 173 fatalities caused by the fire died while attempting to evacuate [111,112], demonstrating that remaining

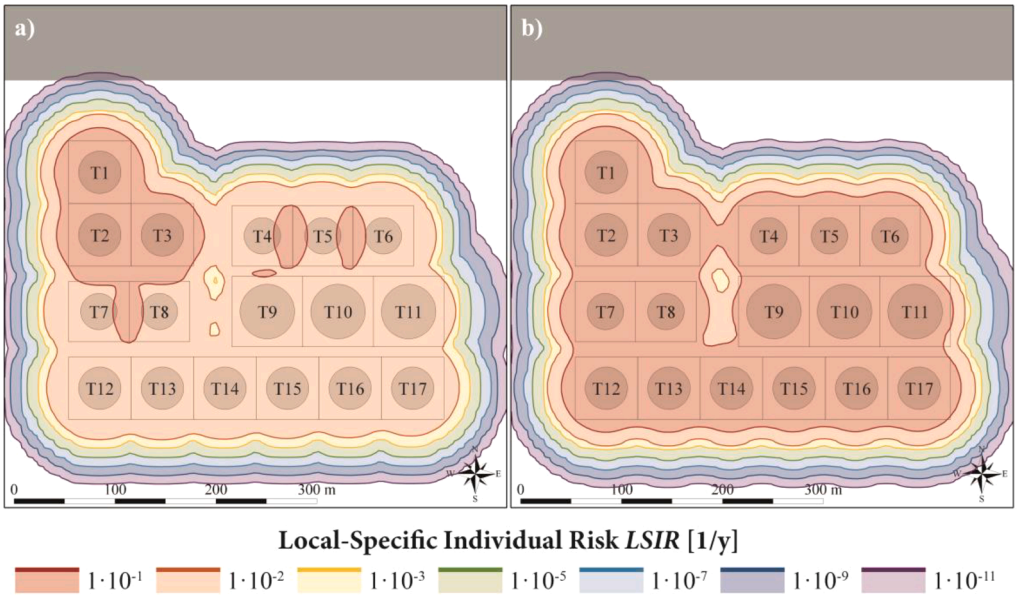


**Fig. 10.** Local-Specific Individual Risk (LSIR) of the wildfire-induced Natech scenarios and the related domino effects considering Case 1 (a) and Case 2 (b).

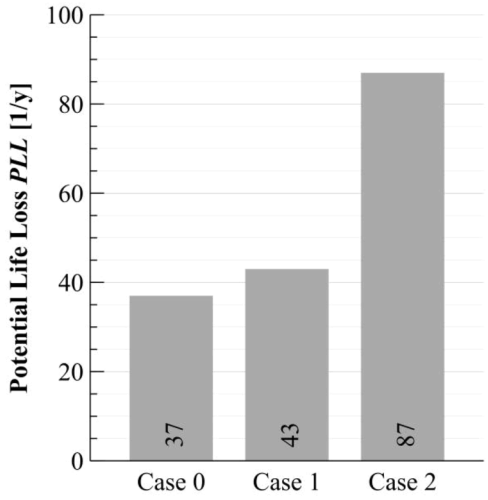


**Fig. 11.** Potential Life Loss calculated for the case studies defined in Section 3.

in the area affected by the fire may be safer than striving for a last-minute evacuation, potentially encountering dangerous conditions in the process. Whittaker and co-workers analyzed the possible causes and identified the delays in warning dissemination and in the implementation of evacuation advice as the main influencing factors [57]. Thus, the risk figures obtained are important to benchmark the risk to which the population is exposed when evacuation or safe sheltering are not possible.

## 6. Conclusions

A dynamic methodology was developed for the vulnerability assessment of atmospheric tank farms to Natech events triggered by wildfires and interface fires. The methodology considers the specific behavior and the intrinsic dynamic features of wildfire events and of the resulting cascading scenarios. An original approach based on the description of the temporal evolution of the chain of events triggered by wildfires is introduced to assess the overall scenarios and to calculate the vulnerability of the site and of each equipment item considered. The methodology also considers the synergistic effect of simultaneous fires and cascading sequences. The comparison with previous methodologies evidences that accounting for the dynamic features is crucial to obtain sound vulnerability figures for Natech events triggered by wildfires and interface fires. Moreover, the results remark the importance of accounting for the harsh conditions generated by the wildfire when assessing emergency response in a chemical site. In perspective, the developed methodology provides a further tool to support the holistic assessment of vulnerability and risk generated by Natech scenarios in the framework of climate change.

## CRediT authorship contribution statement

**Federica Ricci:** Conceptualization, Methodology, Investigation, Data curation, Writing – original draft. **Alessio Misuri:** Conceptualization, Methodology, Investigation. **Giordano Emrys Scarponi:** Conceptualization, Methodology, Writing – original draft. **Valerio Cozzani:** Writing – review & editing, Supervision, Investigation, Conceptualization. **Micaela Demichela:** Conceptualization, Writing – review & editing.

## Declaration of Competing Interest

The authors declare that they have no known competing financial interests or personal relationships that could have appeared to influence the work reported in this paper.

## Data availability

Data will be made available on request.

## References

[1] Nascimento KRDS, Alencar MH. Management of risks in natural disasters: A systematic review of the literature on NATECH events. J Loss Prev Process Ind 2016;44:347–59. https://doi.org/10.1016/j.jlp.2016.10.003.
[2] Suarez-Paba MC, Perreur M, Munoz F, Cruz AM. Systematic literature review and qualitative meta-analysis of Natech research in the past four decades. Saf Sci 2019;116:58–77. https://doi.org/10.1016/j.ssci.2019.02.033.
[3] Cruz AM, Steinberg LJ. Industry Preparedness for Earthquakes and Earthquake-Triggered Hazmat Accidents in the 1999 Kocaeli Earthquake. Earthquake Spectra 2005;21:285–303. https://doi.org/10.1193/1.1889442.

[4] Krausmann E, Cruz AM. Impact of the 11 March 2011, Great East Japan earthquake and tsunami on the chemical industry. Natural Hazards 2013;67:811–28. https://doi.org/10.1007/s11069-013-0607-0.

[5] Misuri A, Cruz AM, Park H, Garnier E, Ohtsu N, Hokugo A, et al. Technological accidents caused by floods: The case of the Saga prefecture oil spill, Japan 2019. International Journal of Disaster Risk Reduction 2021;66:102634. https://doi.org/10.1016/j.ijdrr.2021.102634.

[6] Misuri A, Casson Moreno V, Quddus N, Cozzani V. Lessons learnt from the impact of hurricane Harvey on the chemical and process industry. Reliab Eng Syst Saf 2019;190:106521. https://doi.org/10.1016/j.ress.2019.106521.

[7] Showalter PS, Myers MF. Natural Disasters in the United States as Release Agents of Oil, Chemicals, or Radiological Materials Between 1980-1989: Analysis and Recommendations. Risk Analysis 1994;14:169–82. https://doi.org/10.1111/j.1539-6924.1994.tb00042.x.

[8] Girgin S. The natech events during the 17 August 1999 Kocaeli earthquake: aftermath and lessons learned. Natural Hazards and Earth System Sciences 2011;11:1129–40. https://doi.org/10.5194/nhess-11-1129-2011.

[9] Krausmann E, Renni E, Campedel M, Cozzani V. Industrial accidents triggered by earthquakes, floods and lightning: lessons learned from a database analysis. Natural Hazards 2011;59:285–300. https://doi.org/10.1007/s11069-011-9754-3.

[10] Rasmussen K. Natural events and accidents with hazardous materials. J Hazard Mater 1995;40:43–54. https://doi.org/10.1016/0304-3894(94)00079-V.

[11] Casson Moreno V, Ricci F, Sorichetti R, Misuri A, Cozzani V. Analysis of past accidents triggered by natural events in the chemical and process industry. Chem Eng Trans 2019;74:1405–10. https://doi.org/10.3303/CET1974235.

[12] Luo X, Cruz AM, Tzioutzios D. Extracting Natech Reports from Large Databases: Development of a Semi-Intelligent Natech Identification Framework. International Journal of Disaster Risk Science 2020;11:735–50. https://doi.org/10.1007/s13753-020-00314-6.

[13] Ricci F, Casson Moreno V, Cozzani V. A comprehensive analysis of the occurrence of Natech events in the process industry. Process Safety and Environmental Protection 2021;147:703–13. https://doi.org/10.1016/j.psep.2020.12.031.

[14] Centre for Research on the Epidemiology of Disasters. EM-DAT: The Emergency Events Database. Université Catholique de Louvain (UCL) 2023.

[15] WHO. Chemical releases caused by natural hazard events and disasters: information for public health authorities. Geneva; 2018.

[16] Intergovernmental Panel on Climate Change. Managing the Risks of Extreme Events and Disasters to Advance Climate Change Adaptation. editors. In: Field CB, Barros V, Stocker TF, Qin D, Dokken DJ, Ebi KL, et al., editors. A Special Report of Working Groups I and II of the Intergovernmental Panel on Climate Change. Cambridge, UK, and New York, NY, USA: Cambridge University Press; 2012. p. 594.

[17] Ricci F, Casson Moreno V, Cozzani V. Natech accidents triggered by cold waves. Process Safety and Environmental Protection 2023;173:106–19. https://doi.org/10.1016/j.psep.2023.03.022.

[18] Ricci F, Casson Moreno V, Cozzani V. Natech Accidents Triggered by Heat Waves. Safety 2023;9:33. https://doi.org/10.3390/safety9020033.

[19] Jolly WM, Cochrane MA, Freeborn PH, Holden ZA, Brown TJ, Williamson GJ, et al. Climate-induced variations in global wildfire danger from 1979 to 2013. Nat Commun 2015;6:7537. https://doi.org/10.1038/ncomms8537.

[20] Abatzoglou JT, Kolden CA. Relationships between climate and macroscale area burned in the western United States. Int J Wildland Fire 2013;22:1003. https://doi.org/10.1071/WF13019.

[21] Flannigan MD, Wotton BM, Marshall GA, de Groot WJ, Johnston J, Jurko N, et al. Fuel moisture sensitivity to temperature and precipitation: climate change implications. Clim Change 2016;134:59–71. https://doi.org/10.1007/s10584-015-1521-0.

[22] Westerling AL, Hidalgo HG, Cayan DR, Swetnam TW. Warming and Earlier Spring Increase Western U.S. Forest Wildfire Activity. Science 2006;313:940–3. https://doi.org/10.1126/science.1128834. 1979.

[23] Dennison PE, Brewer SC, Arnold JD, Moritz MA. Large wildfire trends in the western United States, 1984-2011. Geophys Res Lett 2014;41:2928–33. https://doi.org/10.1002/2014GL059576.

[24] Littell JS, McKenzie D, Peterson DL, Westerling AL. Climate and wildfire area burned in western U.S. ecoprovinces, 1916–2003. Ecological Applications 2009;19:1003–21. https://doi.org/10.1890/07-1183.1.

[25] Williams AP, Abatzoglou JT. Recent Advances and Remaining Uncertainties in Resolving Past and Future Climate Effects on Global Fire Activity. Curr Clim Change Rep 2016;2:1–14. https://doi.org/10.1007/s40641-016-0031-0.

[26] Kasischke ES, Turetsky MR. Recent changes in the fire regime across the North American boreal region—Spatial and temporal patterns of burning across Canada and Alaska. Geophys Res Lett 2006;33:L09703. https://doi.org/10.1029/2006GL025677.

[27] Kelly R, Chipman ML, Higuera PE, Stefanova I, Brubaker LB, Hu FS. Recent burning of boreal forests exceeds fire regime limits of the past 10,000 years. Proceedings of the National Academy of Sciences 2013;110:13055–60. https://doi.org/10.1073/pnas.1305069110.

[28] National Interagency Fire Center (NIFC). Fire Information - Statistics - Wildfires and Acres 2022. https://www.nifc.gov/fire-information/statistics/wildfires.

[29] Paveglio TB, Moseley C, Carroll MS, Williams DR, Davis EJ, Fischer AP. Categorizing the Social Context of the Wildland Urban Interface: Adaptive Capacity for Wildfire and Community "Archetypes. Forest Science 2015;61:298–310. https://doi.org/10.5849/forsci.14-036.

[30] Wigtil G, Hammer RB, Kline JD, Mockrin MH, Stewart SI, Roper D, et al. Places where wildfire potential and social vulnerability coincide in the coterminous United States. Int J Wildland Fire 2016;25:896. https://doi.org/10.1071/WF15109.

[31] Manzello SL, Blanchi R, Gollner MJ, Gorham D, McAllister S, Pastor E, et al. Summary of workshop large outdoor fires and the built environment. Fire Saf J 2018;100:76–92. https://doi.org/10.1016/j.firesaf.2018.07.002.

[32] Murphy K, Rich T, Sexton T. An Assessment of Fuel Treatment Effects on Fire Behavior, Suppression Effectiveness, and Structure Ignition on the Angora Fire. 2007.

[33] Rehm RG, Mell W. A simple model for wind effects of burning structures and topography on wildland–urban interface surface-fire propagation. Int J Wildland Fire 2009;18:290. https://doi.org/10.1071/WF08087.

[34] Scarponi GE, Pastor E, Planas E, Cozzani V. Analysis of the impact of wildland-urban-interface fires on LPG domestic tanks. Saf Sci 2020;124:104588. https://doi.org/10.1016/j.ssci.2019.104588.

[35] Scarponi GE, Landucci G, Heymes F, Cozzani V. Experimental and numerical study of the behavior of LPG tanks exposed to wildland fires. Process Safety and Environmental Protection 2018;114:251–70. https://doi.org/10.1016/j.psep.2017.12.013.

[36] Abbasi T, Abbasi SA. The boiling liquid expanding vapour explosion (BLEVE): Mechanism, consequence assessment, management. J Hazard Mater 2007;141:489–519. https://doi.org/10.1016/j.jhazmat.2006.09.056.

[37] Landucci G, Gubinelli G, Antonioni G, Cozzani V. The assessment of the damage probability of storage tanks in domino events triggered by fire. Accid Anal Prev 2009;41:1206–15. https://doi.org/10.1016/j.aap.2008.05.006.

[38] Leslie Irmrm, Birk Amm. State of the art review of pressure liquefied gas container failure modes and associated projectile hazards. J Hazard Mater 1991;28:329–65. https://doi.org/10.1016/0304-3894(91)87083-E.

[39] Moodie K, Cowley LT, Denny RB, Small LM, Williams I. Fire engulfment tests on a 5 tonne LPG tank. J Hazard Mater 1988;20:55–71. https://doi.org/10.1016/0304-3894(88)87006-7.

[40] Boletín Oficial del Estado. Real Decreto 2085/1994, de 20 de octubre, por el que se aprueba el Reglamento de Instalaciones Petroliferas. Boe 1994:39103–5.

[41] Gazzetta Ufficiale della Repubblica Italiana (GURI). Decreto Ministeriale del 13 ottobre 1994. Approvazione della regola tecnica di prevenzione incendi per la progettazione, la costruzione, l'installazione e l'esercizio dei depositi di G.P.L. in serbatoi fissi di capacità complessiva superiore a 5 m3 e/o in. 1994.

[42] Gazzetta Ufficiale della Repubblica Italiana (GURI). Regio Decreto 20 luglio 1934, n. 1303. Approvazione del regolamento per l'esecuzione del R. decreto-legge 2 novembre 1933, n. 1741, che disciplina l'importazione, la lavorazione, il deposito e la distribuzione degli oli minerali e dei loro residui. (034U1. 1934.

[43] Health and Safety Executive (HSE). The storage of flammable liquids in tanks HSG176. 2015. 10.1108/10650741211192046.

[44] National Fire Protection Association (NFPA). NFPA 30. Flammable and Combustible Liquids Code 2018.

[45] Ricci F, Scarponi GE, Pastor E, Planas E, Cozzani V. Safety distances for storage tanks to prevent fire damage in Wildland-Industrial Interface. Process Safety and Environmental Protection 2021;147:693–702. https://doi.org/10.1016/j.psep.2021.01.002.

[46] Cozzani V, Antonioni G, Landucci G, Tugnoli A, Bonvicini S, Spadoni G. Quantitative assessment of domino and NaTech scenarios in complex industrial areas. J Loss Prev Process Ind 2014;28:10–22. 10.1016/j.jlp.2013.07.009.

[47] Antonioni G, Landucci G, Necci A, Gheorghiu D, Cozzani V. Quantitative assessment of risk due to NaTech scenarios caused by floods. Reliab Eng Syst Saf 2015;142:334–45. https://doi.org/10.1016/j.ress.2015.05.020.

[48] Antonioni G, Spadoni G, Cozzani V. A methodology for the quantitative risk assessment of major accidents triggered by seismic events. J Hazard Mater 2007;147:48–59. https://doi.org/10.1016/j.jhazmat.2006.12.043.

[49] Necci A, Antonioni G, Bonvicini S, Cozzani V. Quantitative assessment of risk due to major accidents triggered by lightning. Reliab Eng Syst Saf 2016;154:60–72. https://doi.org/10.1016/j.ress.2016.05.009.

[50] Khakzad N. Modeling wildfire spread in wildland-industrial interfaces using dynamic Bayesian network. Reliab Eng Syst Saf 2019;189:165–76. https://doi.org/10.1016/j.ress.2019.04.006.

[51] Khakzad N, Dadashzadeh M, Reniers G. Quantitative assessment of wildfire risk in oil facilities. J Environ Manage 2018;223:433–43. https://doi.org/10.1016/j.jenvman.2018.06.062.

[52] Sayarshad HR, Ghorbanloo R. Evaluating the resilience of electrical power line outages caused by wildfires. Reliab Eng Syst Saf 2023;240:109588. https://doi.org/10.1016/j.ress.2023.109588.

[53] Arango E, Nogal M, Yang M, Sousa HS, Stewart MG, Matos JC. Dynamic thresholds for the resilience assessment of road traffic networks to wildfires. Reliab Eng Syst Saf 2023;238:109407. https://doi.org/10.1016/j.ress.2023.109407.

[54] Ricci F, Scarponi GEGE, Pastor E, Muñoz JA, Planas E, Cozzani V. Vulnerability of Industrial Storage Tanks to Wildfire: a Case Study. Chem Eng Trans 2021;86:235–40. https://doi.org/10.3303/CET2186040.

[55] Ricci F, Scarponi GE, Pastor E, Planas E, Cozzani V. Asset Integrity in the Case of Wildfires at Wildland-Industrial Interfaces. Chem Eng Trans 2022;90:247–52. https://doi.org/10.3303/CET22290042.

[56] MdT Amin, Scarponi GE, Cozzani V, Khan F. Improved pool fire-initiated domino effect assessment in atmospheric tank farms using structural response. Reliab Eng Syst Saf 2024;242:109751. https://doi.org/10.1016/j.ress.2023.109751.

[57] Whittaker J, Blanchi R, Haynes K, Leonard J, Opie K. Experiences of sheltering during the Black Saturday bushfires: Implications for policy and research. International Journal of Disaster Risk Reduction 2017;23:119–27. https://doi.org/10.1016/j.ijdrr.2017.05.002.

[58] Naderpour M, Rizeei HM, Khakzad N, Pradhan B. Forest fire induced Natech risk assessment: A survey of geospatial technologies. Reliab Eng Syst Saf 2019;191:106558. https://doi.org/10.1016/j.ress.2019.106558.

[59] Lozano FJ, Suárez-Seoane S, Kelly M, Luis E. A multi-scale approach for modeling fire occurrence probability using satellite data and classification trees: A case study in a mountainous Mediterranean region. Remote Sens Environ 2008;112:708–19. https://doi.org/10.1016/j.rse.2007.06.006.

[60] You W, Lin L, Wu L, Ji Z, Yu J, Zhu J, et al. Geographical information system-based forest fire risk assessment integrating national forest inventory data and analysis of its spatiotemporal variability. Ecol Indic 2017;77:176–84. https://doi.org/10.1016/j.ecolind.2017.01.042.

[61] Sakr GE, Elhajj IH, Mitri G, Wejinya UC. Artificial intelligence for forest fire prediction. In: 2010 IEEE/ASME International Conference on Advanced Intelligent Mechatronics. IEEE; 2010. p. 1311–6. https://doi.org/10.1109/AIM.2010.5695809.

[62] Sitanggang IS, Yaakob R, Mustapha N, Ainuddin AN. Predictive Models for Hotspots Occurrence using Decision Tree Algorithms and Logistic Regression. Journal of Applied Sciences 2013;13:252–61. https://doi.org/10.3923/jas.2013.252.261.

[63] Sachdeva S, Bhatia T, Verma AK. GIS-based evolutionary optimized Gradient Boosted Decision Trees for forest fire susceptibility mapping. Natural Hazards 2018;92:1399–418. https://doi.org/10.1007/s11069-018-3256-5.

[64] Vakalis D, Sarimveis H, Kiranoudis C, Alexandridis A, Bafas G. A GIS based operational system for wildland fire crisis management I. Mathematical modelling and simulation. Appl Math Model 2004;28:389–410. https://doi.org/10.1016/j.apm.2003.10.005.

[65] Barber J, Bose C, Bourlioux A, Braun J, Brunelle E, Bryce R, et al. PROMETHEUS - Canada's Wildfire Growth Simulator. 2007.

[66] Hilton J, Hetherton L, Miller C, Sullivan A, Prakash M. The Spark Framework. 2014.

[67] Finney MA. FARSITE: Fire Area Simulator - Model Development and Evaluation. USDA Forest Service - Research Papers RMRS 1998:1–36. https://doi.org/10.2737/RMRS-RP-4.

[68] National Institute of Standards and Technology (NIST). Wildland Urban Interface Fire Dynamics Simulator (WFDS) 2018.

[69] Zárate L, Arnaldos J, Casal J. Establishing safety distances for wildland fires. Fire Saf J 2008;43:565–75. https://doi.org/10.1016/j.firesaf.2008.01.001.

[70] Butler BW, Cohen JD. Firefighter Safety Zones: a Theorical Model Based on Radiative Heating. Int J Wildland Fire 1998;8:73–7.

[71] Heymes F, Aprin L, Forestier S, Slangen P, Baptiste Jarry J, François H, et al. Impact of a distant wildland fire on an LPG tank. Fire Saf J 2013;61:100–7. https://doi.org/10.1016/j.firesaf.2013.08.003.

[72] Anderson W, Pastor E, Butler B, Catchpole E, Dupuy J-L, Fernandes P, et al. Evaluating models to estimate flame characteristics for free-burning fires using laboratory and field data. For Ecol Manage 2006;234:S77. https://doi.org/10.1016/j.foreco.2006.08.113.

[73] Wotton BM, Gould JS, McCaw WL, Cheney NP, Taylor SW. Flame temperature and residence time of fires in dry eucalypt forest. Int J Wildland Fire 2012;21:270. https://doi.org/10.1071/WF10127.

[74] Finney MA, Cohen JD, Forthofer JM, McAllister SS, Gollner MJ, Gorham DJ, et al. Role of buoyant flame dynamics in wildfire spread. Proceedings of the National Academy of Sciences 2015;112:9833–8. https://doi.org/10.1073/pnas.1504498112.

[75] Billaud Y, Kaiss A, Consalvi J-L, Porterie B. Monte Carlo estimation of thermal radiation from wildland fires. International Journal of Thermal Sciences 2011;50:2–11. https://doi.org/10.1016/j.ijthermalsci.2010.09.010.

[76] Bakhshaii A, Johnson EA. A review of a new generation of wildfire–atmosphere modeling. Canadian Journal of Forest Research 2019;49:565–74. https://doi.org/10.1139/cjfr-2018-0138.

[77] Or D, Furtak-Cole E, Berli M, Shillito R, Ebrahimian H, Vahdat-Aboueshagh H, et al. Review of wildfire modeling considering effects on land surfaces. Earth Sci Rev 2023;245:104569. https://doi.org/10.1016/j.earscirev.2023.104569.

[78] Mudan KS. Geometric view factors for thermal radiation hazard assessment. Fire Saf J 1987;12. https://doi.org/10.1016/0379-7112(87)90024-5.

[79] Mannan S. Lees' loss prevention in the process industries. 3rd ed. Oxford, UK: Elsevier Butterworth-Heinemann; 2005.

[80] Zhou J, Reniers G, Cozzani V. Improved probit models to assess equipment failure caused by domino effect accounting for dynamic and synergistic effects of multiple fires. Process Safety and Environmental Protection 2021;154:306–14. https://doi.org/10.1016/j.psep.2021.08.020.

[81] Ding L, Khan F, Abbassi R, Ji J. FSEM: An approach to model contribution of synergistic effect of fires for domino effects. Reliab Eng Syst Saf 2019;189:271–8. https://doi.org/10.1016/j.ress.2019.04.041.

[82] Cozzani V, Gubinelli G, Antonioni G, Spadoni G, Zanelli S. The assessment of risk caused by domino effect in quantitative area risk analysis. J Hazard Mater 2005;127:14–30. https://doi.org/10.1016/j.jhazmat.2005.07.003.

[83] Landucci G, Argenti F, Tugnoli A, Cozzani V. Quantitative assessment of safety barrier performance in the prevention of domino scenarios triggered by fire. Reliab Eng Syst Saf 2015;143:30–43. https://doi.org/10.1016/j.ress.2015.03.023.

[84] Landucci G, Bonvicini S, Cozzani V. A methodology for the analysis of domino and cascading events in Oil & Gas facilities operating in harsh environments. Saf Sci 2017;95:182–97. https://doi.org/10.1016/j.ssci.2016.12.019.

[85] Bucelli M, Landucci G, Haugen S, Paltrinieri N, Cozzani V. Assessment of safety barriers for the prevention of cascading events in oil and gas offshore installations operating in harsh environment. Ocean Engineering 2018;158:171–85. https://doi.org/10.1016/j.oceaneng.2018.02.046.

[86] Van Den Bosh CJHJH, Weterings RAPM. Methods for the calculation of physical effects due to releases of hazardous materials (liquids and gases) (Yellow Book). third. The Hague (NL): Committee for the Prevention of Disasters; 2005.

[87] Center for Chemical Process Safety (CCPS). Guidelines for chemical process quantitative risk analysis. New York: American Institute of Chemical Engineers - Center of Chemical Process Safety; 1990.

[88] Landucci G, Necci A, Antonioni G, Argenti F, Cozzani V. Risk assessment of mitigated domino scenarios in process facilities. Reliab Eng Syst Saf 2017;160:37–53. https://doi.org/10.1016/j.ress.2016.11.023.

[89] Misuri A, Landucci G, Cozzani V. Assessment of risk modification due to safety barrier performance degradation in Natech events. Reliab Eng Syst Saf 2021;212:107634. https://doi.org/10.1016/j.ress.2021.107634.

[90] Misuri A, Antonioni G, Cozzani V. Quantitative risk assessment of domino effect in Natech scenarios triggered by lightning. J Loss Prev Process Ind 2020;64:104095. https://doi.org/10.1016/j.jlp.2020.104095.

[91] Freeman RA. CCPS guidelines for chemical process quantitative risk analysis. Plant/Operations Progress 1990;9:231–5. https://doi.org/10.1002/prsb.720090409.

[92] Van Den Bosh CJH. Methods for the Determination of Possible Damage to People and Objects Resulting from Releases of Hazardous Materials (Green Book). The Hague (NL): Committee for the Prevention of Disasters; 1992.

[93] Zanobetti F, Pio G, Jafarzadeh S, Ortiz MM, Cozzani V. Inherent safety of clean fuels for maritime transport. Process Safety and Environmental Protection 2023;174:1044–55. https://doi.org/10.1016/j.psep.2023.05.018.

[94] Tugnoli A, Landucci G, Cozzani V. Key performance indicators for inherent safety: Application to the hydrogen supply chain. Process Safety Progress 2009;28:156–70. https://doi.org/10.1002/prs.10303.

[95] Tugnoli A, Cozzani V, Landucci G. A consequence based approach to the quantitative assessment of inherent safety. AIChE Journal 2007;53:3171–82. https://doi.org/10.1002/aic.11315.

[96] Gao P, Terando AJ, Kupfer JA, Morgan Varner J, Stambaugh MC, Lei TL, et al. Robust projections of future fire probability for the conterminous United States. Science of The Total Environment 2021;789:147872. https://doi.org/10.1016/j.scitotenv.2021.147872.

[97] Guyette RP, Stambaugh MC, Dey DC, Muzika R-M. Predicting Fire Frequency with Chemistry and Climate. Ecosystems 2012;15:322–35. https://doi.org/10.1007/s10021-011-9512-0.

[98] Thompson MP, Calkin DE, Finney MA, Ager AA, Gilbertson-Day JW. Integrated national-scale assessment of wildfire risk to human and ecological values. Stochastic Environmental Research and Risk Assessment 2011;25:761–80. https://doi.org/10.1007/s00477-011-0461-0.

[99] Uijt de Haag PAM, Ale BJM. Guidelines for Quantitative Risk Assessment (Purple book). The Hague (NL): Committee for the Prevention of Disasters; 2005.

[100] Carter DA, Hirst IL. Worst case methodology for the initial assessment of societal risk from proposed major accident installations. J Hazard Mater 2000;71:117–28. https://doi.org/10.1016/S0304-3894(99)00075-8.

[101] Hirst I, Carter DA. A "worst case" methodology for obtaining a rough but rapid indication of the societal risk from a major accident hazard installation. J Hazard Mater 2002;92:223–37. https://doi.org/10.1016/S0304-3894(02)00016-X.

[102] Okrent D, Dunster HJ, Van Reijen G. Industrial risks. Proceedings of the Royal Society of London A Mathematical and Physical Sciences 1981;376:133–49. https://doi.org/10.1098/rspa.1981.0081.

[103] Misuri A, Ricci F, Sorichetti R, Cozzani V. The Effect of Safety Barrier Degradation on the Severity of Primary Natech Scenarios. Reliab Eng Syst Saf 2023;235:109272. https://doi.org/10.1016/j.ress.2023.109272.

[104] Misuri A, Landucci G, Cozzani V. Assessment of safety barrier performance in the mitigation of domino scenarios caused by Natech events. Reliab Eng Syst Saf 2021;205:107278. https://doi.org/10.1016/j.ress.2020.107278.

[105] Misuri A, Landucci G, Cozzani V. Assessment of safety barrier performance in Natech scenarios. Reliab Eng Syst Saf 2020;193:106597. https://doi.org/10.1016/j.ress.2019.106597.

[106] Krausmann E, Cruz AM. Past Natech Events. Natech Risk Assessment and Management. Elsevier; 2017. p. 3–31. https://doi.org/10.1016/B978-0-12-803807-9.00002-4.

[107] Krausmann E, Salzano E. Lessons Learned From Natech Events. Natech Risk Assessment and Management, Elsevier 2017:33–52. https://doi.org/10.1016/B978-0-12-803807-9.00003-6.

[108] Lindell MK, Perry RW. Identifying and managing conjoint threats: Earthquake-induced hazardous materials releases in the US. J Hazard Mater 1996;50:31–46. https://doi.org/10.1016/0304-3894(96)01764-5.

[109] Ricci F, Yang M, Reniers G, Cozzani V. The Role of Emergency Response in Risk Management of Cascading Events Caused by Natech Accidents. Chem Eng Trans 2022;91:361–6. https://doi.org/10.3303/CET2291061.

[110] Lindell MK, Perry RW. Earthquake Impacts and Hazard Adjustment by Acutely Hazardous Materials Facilities following the Northridge Earthquake. Earthquake Spectra 1998;14:285–99. https://doi.org/10.1193/1.1586000.

[111] Blanchi R, Leonard J, Haynes K, Opie K, James M, de Oliveira FD. Environmental circumstances surrounding bushfire fatalities in Australia 1901–2011. Environ Sci Policy 2014;37:192–203. https://doi.org/10.1016/j.envsci.2013.09.013.

[112] Haynes K, Handmer J, McAneney J, Tibbits A, Coates L. Australian bushfire fatalities 1900–2008: exploring trends in relation to the 'Prepare, stay and defend or leave early' policy. Environ Sci Policy 2010;13:185–94. https://doi.org/10.1016/j.envsci.2010.03.002.